3552–3578 *Nucleic Acids Research, 2018, Vol. 46, No. 7* *Published online 5 March 2018*
doi: 10.1093/nar/gky109

The yeast Ty1 retrotransposon requires components of the nuclear pore complex for transcription and genomic integration

Savrina Manhas[1], Lina Ma[2] and Vivien Measday[1,2,*]

[1]Department of Biochemistry and Molecular Biology, 2350 Health Sciences Mall, Life Sciences Centre, Faculty of Medicine, University of British Columbia, Vancouver, British Columbia, V6T 1Z3, Canada and [2]Wine Research Centre, 2205 East Mall, Faculty of Land and Food Systems, University of British Columbia, Vancouver, British Columbia, V6T 1Z4, Canada

Received June 23, 2016; Revised February 01, 2018; Editorial Decision February 02, 2018; Accepted February 26, 2018

ABSTRACT

Nuclear pore complexes (NPCs) orchestrate cargo between the cytoplasm and nucleus and regulate chromatin organization. NPC proteins, or nucleoporins (Nups), are required for human immunodeficiency virus type 1 (HIV-1) gene expression and genomic integration of viral DNA. We utilize the Ty1 retrotransposon of *Saccharomyces cerevisiae* (*S. cerevisiae*) to study retroviral integration because retrotransposons are the progenitors of retroviruses and have conserved integrase (IN) enzymes. Ty1-IN targets Ty1 elements into the genome upstream of RNA polymerase (Pol) III transcribed genes such as transfer RNA (tRNA) genes. Evidence that *S. cerevisiae* tRNA genes are recruited to NPCs prompted our investigation of a functional role for the NPC in Ty1 targeting into the genome. We find that Ty1 mobility is reduced in multiple Nup mutants that cannot be accounted for by defects in Ty1 gene expression, cDNA production or Ty1-IN nuclear entry. Instead, we find that Ty1 insertion upstream of tRNA genes is impaired. We also identify Nup mutants with wild type Ty1 mobility but impaired Ty1 targeting. The NPC nuclear basket, which interacts with chromatin, is required for both Ty1 expression and nucleosome targeting. Deletion of components of the NPC nuclear basket causes mis-targeting of Ty1 elements to the ends of chromosomes.

INTRODUCTION

An obligate and irreversible step in retroviral replication is insertion of retroviral DNA into the host cell's genome. Host cell machinery, although commonly hijacked by retroviruses for replication, can pose challenges to genomic insertion of retroviral genetic material. One such cellular structure, the nuclear envelope (NE), surrounds the nucleus creating a physical barrier between retroviruses and their target genomic DNA. In mammalian cells, the NE breaks down during mitosis allowing retroviruses, such as Moloney Murine Leukemia Virus, access to genomic DNA for integration (1,2). However, Human Immunodeficiency Virus Type 1 (HIV-1) can productively infect non-dividing, terminally differentiated cells, and therefore, has a mechanism to overcome the NE barrier to gain access to genomic integration sites (3,4). Because the yeast *Saccharomyces cerevisiae* (*S. cerevisiae*) NE does not break down during mitosis, retrotransposons in yeast and HIV-1 may possess similar mechanisms to access chromatin.

The *S. cerevisiae* Ty1 retrotransposon, which is a member of the Ty1/*copia* family, resembles a retrovirus in structure and life cycle except that Ty1 does not have an extracellular phase (5). The Ty1 element consists of *GAG* and *POL* open reading frames (ORFs) flanked on either side by long terminal repeat (LTR) sequences (5). *GAG* encodes a structural protein of the virus-like particle (VLP), while *POL* produces the enzymes protease (PR), integrase (IN), reverse transcriptase (RT) and ribonuclease H (RH) (5). Early stages in Ty1 replication include Ty1 transcription, translation, VLP assembly, Ty1 Gag and Pol processing followed by reverse transcription of the Ty1 mRNA intermediate to complementary DNA (cDNA). The newly synthesized Ty1 cDNA forms a complex with IN called a pre-integration complex (PIC) (5). The PIC localizes to the nucleus where Ty1 cDNA is inserted upstream of genes transcribed by RNA polymerase III (RNA Pol III), such as transfer RNA (tRNA) genes by a mechanism that depends on Ty1-IN (6). Recently we, and Bridier-Nahmias *et al.*, discovered that Ty1-IN interacts with RNA Pol III subunits and that this interaction is necessary for targeting Ty1 element insertion upstream RNA Pol III transcribed genes (7,8).

*To whom correspondence should be addressed. Tel: +1 604 827 5744; Fax: +1 604 822 5143; Email: vmeasday@mail.ubc.ca
Present address: Vivien Measday, Wine Research Centre, University of British Columbia, Room 325-2205 East Mall, Vancouver, British Columbia V6T 1Z4 Canada.

To translocate across the NPC, soluble transport factors (karyopherins/importins/exportins) recognize protein cargoes carrying a nuclear localization signal (NLS) for import substrates or a nuclear export signal for export substrates. Ty1-IN has a bipartite NLS that is required for entry into the nucleus and binds the importin-alpha transporter (Kap60), suggesting that Ty1-IN uses the classical nuclear import pathway for nuclear entry (9–11). It is not known if the Ty1 VLP or Ty1 PIC is delivered to the NPC or how the Ty1 PIC travels through the NPC. As well, the role of NPC proteins, termed nucleoporins (Nups), in Ty1 integration remains unknown but potentially significant given the emerging role for Nups in gene regulation and chromatin organization as well as retroviral integration (12,13).

The NE is studded with NPCs that orchestrate macromolecular movement of cargo to and from the nucleus. Small molecules can passively diffuse across the NE while macromolecules pass through by interacting directly with NPCs or soluble transport factors (14). The yeast NPC is composed of circa 30 different Nups configured into multiple sub-complexes that form the interacting structural layers of the NPC (Figure 1A) (15,16). The central channel, where molecular exchange occurs, is composed of central phenylalanine-glycine (FG) repeat Nups (Nsp1, Nup49, Nup57, Nup100, Nup116, Nup145N) (15,16). The outer ring Nup84 subcomplex (Nup84, Nup85, Nup120, Nup133, Nup145C, Sec13, Seh1) and inner ring Nup170 subcomplex (Nup157, Nup170, Nup188, Nup53, Nup59, Nup192) form a core scaffold that the FG Nups attach to (15–19). The NPC has structural asymmetry: on the cytoplasmic face of the NPC are the cytoplasmic Nups (Nup42, Nup159) whereas on the nuclear face Nup1, Nup2, Nup60, Mlp1 and Mlp2 form the nuclear basket (15,16). Nups in the nuclear basket are of particular interest for mediating Ty1 integration given their proximity to chromatin as well as their characterized role in chromatin organization and interaction with actively transcribed genes (13,20–26). The linker Nups (Nic96, Nup82), positioned toward the inside of the channel, connect the inner and outer rings (17) and serve as attachment sites for FG Nups whereas the transmembrane ring Nups (Ndc1, Pom34, Pom152) help anchor the NPC in the NE (15,16). These basic structural components of the NPC are conserved across all eukaryotes (15,16).

Nups have been identified as Ty1 host factors in functional genomics screens. Two outer ring Nups, *NUP84* and *NUP133* were identified as deletion mutants with reduced Ty1 transposition but normal (*nup84Δ*) or increased (*nup133Δ*) levels of Ty1 cDNA indicating that Nup84 and Nup133 affect a late step in retrotransposition (27). *NUP84* was identified in another genome-wide screen for deletion mutants with reduced Ty1 mobility along with *NUP170* (28). A genome-wide screen conducted in a mutant strain background with hyper transposition discovered reduced transposition upon deletion of *NUP133*, *NUP120*, *NUP170* or *NUP188* (29). Although members of both the Nup84 (Nup84, Nup120, Nup133) outer ring and Nup170 (Nup170, Nup188) inner ring subcomplexes have been identified as Ty1 host factors, their specific role in Ty1 mobility remains to be characterized (27–29).

Nups have also been identified as host factors of the *S. cerevisiae* Ty3 LTR retrotransposon that is a member of the Ty3/Gypsy family and also integrates upstream of RNA pol III transcribed genes. Unlike Ty1 which inserts in a ∼1kb window upstream of RNA Pol III transcribed genes, Ty3 inserts 1 to 4 nucleotides upstream of the RNA Pol III transcription start site (30). A screen that monitored Ty3 insertion in a collection of mutants identified 53 genes, of which 3 were Nups (*NUP116*, *NUP159*, *NUP157*), as potential Ty3 host factors (31). Additionally, a screen of *S. cerevisiae* nonessential knockout strains identified 8 nuclear transport mutants (*NUP100*, *NUP84*, *NUP120*, *NUP133*, *NUP59*, *KAP120*, *SAC3*, *NPL3*) with increased or decreased Ty3 transposition (32).

Yeast cells lacking a component of the Nup84 outer ring subcomplex, such as *NUP133* or *NUP120*, display clustering of pores on the NE (33,34). In the *nup133Δ* and *nup120Δ* mutant background, Ty3 VLPs localize to clustered NPCs within 6 h of Ty3 induction (35). The association between Ty3 VLPs and NPC clusters in these mutants argues that Ty3 VLPs interact physically with the NPC during the time that complete Ty3 cDNA products can first be detected. Nups may function in Ty3 VLP docking or uncoating, similar to the role of some Nups in HIV-1 replication. Tf1, an active LTR retrotransposon in the fission yeast *Schizosaccharomyces pombe* (*S. pombe*), encodes Gag, PR, RT and IN proteins that assemble along with copies of RNA to form VLPs (36–38). Nuclear entry of Tf1-Gag and HIV-1 viral protein R (VPR) in *S. pombe* require the FG nucleoporin Nup124 (39–42). Three independent genome-wide small interfering RNA (siRNA) screens for host factors required for HIV-1 replication identified Nups involved in PIC trafficking and integration, thus lending support for the evolutionarily conserved role of Nups in retrotransposon and retroviral life cycles (43–45).

The identification of Nups as potential host factors for Ty1, Ty3, Tf1 and HIV-1 replication along with the identified role of tRNA transcription at NPCs (21) led us to investigate the functional role of NPC proteins in Ty1 replication and genome insertion. In this study, we systematically screen a panel of mutant Nup yeast strains using functional assays for multiple aspects of the Ty1 replication cycle including Ty1 mRNA expression, Ty1 Gag levels, Ty1-IN nuclear localization and Ty1 element genome integration. Given that Ty1 elements preferentially insert upstream of tRNA genes and yeast tRNA genes are recruited to the NPC to couple tRNA gene expression and nuclear export (21), we hypothesized that the NPC may also have an active role in Ty1 element targeting.

Here, we use a Ty1 reporter plasmid to monitor Ty1 mobility, which is the result of IN-mediated retrotransposition of Ty1 to a new genomic location and Ty1 cDNA recombination with a pre-existing genomic Ty1 element, in a panel of Nup mutant yeast strains. We also measure endogenous Ty1 element insertion in these strains using a PCR-based assay. Our findings indicate that deletion or mutation of multiple Nups alters Ty1 mobility and Ty1 element insertion upstream of tRNA genes without affecting the levels of Ty1 replication intermediates (Ty1 mRNA, Gag protein, Ty1 cDNA) and Ty1-IN nuclear localization. We find that deletion of the Nup60 nuclear basket protein reduces

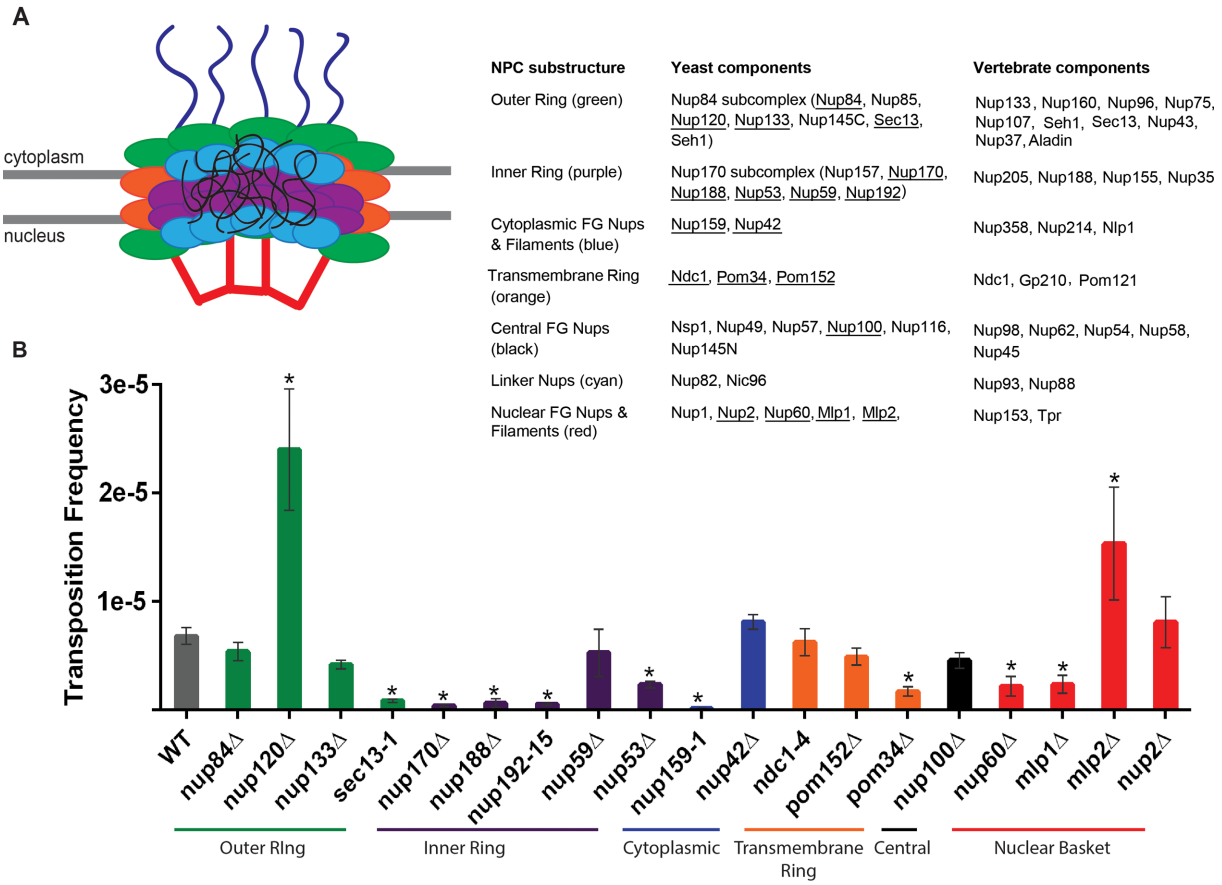

Figure 1. The NPC has a role in Ty1 mobility. (**A**) Major NPC structural subunits adapted from (15,16). The underlined Nups were examined for a role in Ty1 mobility. (**B**) Ty1 transposition frequency of wild type (WT) and 19 Nup mutant strains [outer ring (*nup84Δ, nup120Δ, nup133Δ, sec13–1*), inner ring (*nup170Δ, nup188Δ, nup192–15, nup59Δ, nup53Δ*), cytoplasmic (*nup159–1, nup42Δ*), transmembrane ring (*ndc1–4, pom152Δ, pom34Δ*), central (*nup100Δ*), *nuclear basket* (*nup60Δ, mlp1Δ, mlp2Δ* and *nup2*)] carrying a *CEN* plasmid with a *HIS3AI* tagged Ty1 element expressed from its endogenous promoter (pBDG922). Cells from two colonies, grown in triplicate, were induced to transpose for 5 days at 20°C. A two-tailed *t* test was used for analysis and mutants with a statistically significant difference in transposition frequency from wild type ($P < 0.05$) are marked with an asterisk (*).

Ty1 element mRNA expression and eliminates Ty1 element genome-targeting. However, removal of the N-terminal amphipathic helix (AH) and helical region (HR) of Nup60, which have been recently shown to be required for NE membrane curvature (46), allows for Ty1 expression and targeting upstream of tRNA genes but instead alters the nucleosome pattern of Ty1 element integration. We show that a defect in the typical nucleosome pattern of Ty1 integration also occurs when the AH and HR regions of Nup1, also required for NE membrane curvature, are deleted (46). Nup2, which is a mobile Nup that interacts with Nup60 (47), has a Ran-binding domain (RBD) that we demonstrate is important for Ty1 targeting. Finally, we show that when nuclear basket proteins are deleted, Ty1 elements are re-targeted to subtelomeric regions, similar to an Rpc40 mutant that no longer interacts with Ty1-IN (7). Taken together with the well-defined role of actively transcribed tRNA genes relocating to NPCs, our results suggest that the nuclear basket couples cellular processes such a tRNA expression, Ty1 expression and Ty1 integration.

MATERIALS AND METHODS

Yeast strains, plasmids and media

Both non-essential deletion (Δ) and essential temperature sensitive (ts) mutant yeast strains were previously engineered (48,49). Yeast strains used in this study are listed in Supplementary Table S1 and deletion mutants were verified by colony PCR. *S. cerevisiae* strains were grown in yeast peptone dextrose (YPD), synthetic complete (SC) media or SC media lacking uracil (URA), leucine (LEU) or histidine (HIS) and supplemented with combinations of dextrose (Dex), raffinose (Raf), galactose (Gal) and/or hygromycin B (Invitrogen) as required. The *NUP1* (pRS313-NUP1-mCherry, pRS313-nup1Δ1–32-mCherry, pRS313-nup1Δ85–123-mCherry) and *NUP60* (pRS315-NUP60-mCherry, pRS315-nup60Δ1–47-mCherry, pRS315-nup60Δ48–162-mCherry, pRS315-nup60Δ1–162-mCherry) AH and HR mutant plasmids were a gift from Dr Köhler (46). The following Ty1 expression plasmids were used in this study for Ty1 mobility assays: pBDG922, pBDG924 and pBDG633 from Dr Garfinkel (10,50), and pJBe376 from Dr Boeke for Ty1 insertion PCR with the ΔFG yeast strains.

Ty1 Gag westerns

Yeast strains were grown on selection plates for 3 days at 20°C. For each strain, colonies were transferred to 10 ml of YPD and grown overnight at 20°C to log phase (OD_{600} 0.5–1.0) in duplicate. Cells were pelleted, washed with ice-cold water and then re-suspended in ice-cold lysis buffer (50 mM Tris–HCl pH 7.5, 0.5 mM EDTA pH 8.0, 250 mM NaCl, 0.1% NP40 and protease inhibitors). After glass bead lysis, samples were centrifuged at 14 000 rpm for 10 min and the supernatant [whole cell extract (WCE)] was transferred to a new eppendorf tube. The WCE protein concentration was determined by Bio-Rad Protein Assay. Sodium dodecyl sulfate (SDS) loading dye (2×) was added to 60 μg of each WCE sample, which were then boiled for 3–5 min and loaded on a 12% SDS-PAGE gel and transferred to a methanol activated polyvinylidene difluoride or nitrocellulose membrane using the Bio-Rad Transblot Turbo system (25 V, 2.5 A, 15 min). Membranes were probed with anti-Gag sera (1:15 000, provided by Dr Jeff Boeke) and anti-GAPDH (1:5000, UBC Antibody Lab) as a loading control. Membranes were incubated with the following infrared secondary antibodies from Mandel Scientific: IRDye® 680RD Goat anti-Rabbit IgG (H+L), IRDye® 800CW Goat anti-Mouse IgG (H+L), both at 1:10 000, and imaged on an Odyssey CLx. Ty1 Gag protein levels (p49 and p45) were quantified relative to GAPDH levels using Image Studio Version 2.1 software.

Ty1 mobility quantification assay

This assay was performed as described in (51). Briefly, strains were transformed with a *CEN* based *URA3* marked Ty1-his3-AI reporter plasmid (pBDG922, pBDG924 or pBDG633, all kind gifts from Dr David Garfinkel). Single colonies were isolated and patched. Two thousand cells were inoculated into SC-URA media and grown for 5 days at 20°C. 10^7 cells were plated on SC-URA-HIS plates and 200 cells on SC-URA plates to test for transposition frequency and viability, respectively. After incubation for 2 days at 25°C, the transposition frequency of the marked Ty1 element was calculated by the following formula: # colonies on SC-URA-HIS/10^7 divided by # colonies on SC-URA/200. At least two single colonies were tested in triplicate for each strain. Our Ty1 mobility data does not account for possible changes in plasmid copy numbers due to NPC disruption. Statistical analyses were performed using GraphPad Prism 6.

pPGK1-Ty1-IN-mCherry construction

The *PGK1*-mCherry expression vector (pCW1; BVM460) was a gift from Dr Chris Walkey. pCW1 carries both hygromycin and ampicillin resistance genes and has a single Sal I restriction site between the *PGK1* and mCherry ORFs (52). pCW1 was digested with Sal I and then dephosphorylated with calf intestinal phosphatase. Ty1-IN was amplified from a plasmid carrying a full length Ty1 element called *pGAL1-Ty1-H3* (pJEF724, generous gift from Dr Jef Boeke) with IN-XhoI-F (5′-GGTGGTGTCTCGAGATGAATGTCCATACAAGTGAAAGTACACGCAAA-3′) and IN- XhoI-R (5′-GGTGGTGTCTCGAGTGCAATCAGGTGAATTCGTTTCTTCGATCT-3′) primers which have eight bases in front of Xho I site (underlined). The resulting PCR product was purified, digested with Xho I then ligated with Sal I digested pCW1.

Microscopy

Yeast strains were transformed with pPGK1-Ty1-IN-mCherry or empty vector (pCW1; BVM460) and grown at 25°C on YPD plates supplemented with hygromycin B for 2–3 days. Two isolates per mutant strain were grown to log phase overnight at 25°C in 5 ml of SC media supplemented with hygromycin B and 2% Dex. Thirty minutes prior to imaging, 1 ml of each culture was stained with 0.5 μg Hoechst 33342 (Life Technologies). Live cells were imaged with a Zeiss Axio Observer inverted microscope equipped with a Zeiss Colibri LED illuminator and a Zeiss Axiocam ultrahigh-resolution monochrome digital camera Rev 3.0; ten image stacks were acquired with a 40× objective, at a step of 0.3 μm, and analysed with Zeiss Axiovision software as in (53).

Ty1 cDNA

Ty1 cDNA analysis was generally performed as described (54–56). Briefly, strains were grown in YPD for 2 days at 20°C, followed by genomic DNA extraction using phenol–chloroform. Ten micrograms of genomic DNA was digested with the enzyme PvuII (New England Biolabs) to release a ∼2.4 kb fragment of Ty1 cDNA. Digestion reactions were run on a 0.8% Tris–borate EDTA (TBE) agarose gel and then transferred to a Hybond-XL charged nylon membrane (GE Healthcare). Membranes were subsequently probed with a ^{32}P-α-dATP (Perkin Elmer) radiolabelled 1517 bp PvuII/SnaBI C-terminal fragment of the Ty1 element using a DecaLabel DNA labeling Kit (ThermoScientific). A Typhoon Trio Variable Mode Imager was used for imaging and ImageQuant software was used for quantitation.

Quantitative PCR

Quantitative PCR (qPCR) was performed and analyzed as described (8). Yeast strains were grown in YPD media at 20°C to log phase; 10^7 cells were pelleted and total RNA was isolated with a Qiagen RNeasy kit. The Superscript VILLO cDNA synthesis kit (Invitrogen) was used for cDNA synthesis from 1 μg of RNA. Real-time PCR was set-up in triplicate with 2 μl of a 1:50 cDNA dilution and Power SYBR Green Master Mix (Invitrogen). A standard 2-h comparative PCR analysis was performed using a 7500 Real Time PCR system (Applied Biosystems). The primers for Ty1 mRNA expression were: OVM760: 5′-TCG CATGGTCAGAAGATCGA-3′ and OVM761: 5′-ACC CACAGCAGTGCATGATG-3′. The primers for amplifying mature *tLEU* (CAA) (10 genes) are OVM959 5′- GGTT GTTTGGCCGAGCGGTCTAAG-3′ and OVM960 5′-T GGTTGCTAAGAGATTCGAACTCT-3′ (7). The primers for amplifying unspliced tLEU (CAA) *(tLEU denovo*, 7 genes) are OVM959 5′-GGTTGTTTGGCCGAGCGGT CTAAG-3′ and OVM961 5′-TATTCCCACAGTTAACT GCGGTC-3′ (7). The primers for amplifying mature *tGLY*

(GCC) expression (16 genes) are OVM962 5′-GCGCA AGTGGTTTAGTGG-3′ and OVM963 5′-AAGCCCGGA ATCGAACC-3′ (7). qPCR analysis was performed using the comparative C_T method ($\Delta\Delta C_T$ method, Applied Biosystems), with *TAF10* used as an internal control. The *TAF10* primers were: OVM695 5′-GGCGTGCAGCAGA TTTCAC-3′and OVM696 5′-TGAGCCCGTATTCAGCA ACA-3′ as previously described (8).

SUF16, SUP61 and tGLY Ty1 integration assay

This assay was performed as described (51) with the following modifications. Yeast strains were grown on plates for 3 days at 20°C then colonies were transferred to liquid media and grown for 3 days at 20°C to induce endogenous Ty1 transposition. For the ΔFG Nup mutants (*nup1ΔFxFG*, *nup2ΔFxFG*, *nup60ΔFxF*, *nup1ΔFxFG nup2ΔFxFG*, *nup1ΔFxFG nup2ΔFxFG nup60ΔFxF*), each strain was transformed with a pGAL-TyH3mHIS3AI-URA3 plasmid (pJBe376) and induced in Gal media for 24 h as described (54). Glass beads and lysis buffer [2% Triton X-100, 1% SDS, 100 mM NaCl, 10 mM Tris–HCl (pH 8.0), 1 mM EDTA] were used to lyse cells, and genomic DNA was extracted using phenol–chloroform. Ty1 insertions upstream of the *SUF16* and *SUP61* loci on chromosome III were amplified using *SNR33* out (OVM890 5′-GTGACAC CATCGTACAAAGAGGGC-3′) and *BUD31* out (OSM27 5′-GGCTTGGATCTTCTGGTCTTTATGC-3′) primers, respectively, along with the TyB out: (OVM889 5′-GCT GATGTGATGACAAAACCTCTTCCG-3′) primer (51). Ty insertion upstream of 16 copies of the glycine tRNA gene (GCC anticodon), collectively called *tGLY*, were amplified with OVM807 (5′-GGATTTTACCACTAAACCA CTT-3′) and TyB out (57). The primers were used to amplify Ty1 insertions from 1 μg of genomic DNA using the following touchdown PCR cycling parameters: 96°C, 2 min; 5 cycles at 96°C, 30 s; 70°C, 30 s; 68°C, 1 min followed by 5 cycles at 96°C, 30 s; 67°C, 30 s; 68°C, 1 min followed by 5 cycles at 96°C, 30 s; 65°C, 30 s; 68°C, 1 min followed by 5 cycles at 96°C, 30 s; 63°C, 30 s; 68°C, 1 min followed by 10 cycles at 96°C, 30 s; 60°C, 30 s; 68°C, 1 min. The presence of quality genomic DNA was verified by PCR amplification of the *CPR7* locus with 5 ng of genomic DNA (CPR7-forward: 5′-GTTTGTGATTTATCTCTGGACTG CT-3′ and CPR7-reverse: 5′-AGTTCGTCTCTCCTTCA TATTCTCA-3′) by executing the following PCR parameters: 94°C, 2 min; 30 cycles at 94°C, 30 s; 60°C, 30 s; 72°C, 2 min followed by 72°C, 10 min. Each yeast strain was assayed in triplicate.

Subtelomere PCR assay

This assay was performed as previously described (8) with 1.5 μg of genomic DNA, the TyB out primer (OVM889), and either one of the following primers: OSC66, 5′-CCA AGGATCTAGGTGAGGCTTTGAGAA-3′ (Chr XIV left end 13,634–13,669 bp (*SNZ2*) and Chr VI left end 11,739–11,765 bp (*SNZ3*)); OSC68, 5′-GACATGGGCCCCTGT TGCTTATATTGT-3′ (Chr IV left end 12 021–12 047 bp (*HXT15*) and Chr X right end 733 753–733 779 bp (*HXT16*)). The PCR cycling parameters were identical to the Ty1 integration assay mentioned above apart from the final step which was 15 cycles at 96°C, 30 s; 60°C, 30 s; 63°C, 1 min.

RESULTS

Subunits of the yeast nuclear pore complex are involved in Ty1 mobility

We tested 15 non-essential deletion and 4 essential ts Nup mutant yeast strains for significant changes in Ty1 mobility. Ty1 mobility was quantified by monitoring the formation of HIS+ colonies in NPC mutant yeast strains carrying a plasmid (pBDG922) with a *HIS3* marked Ty1 element (50). The *HIS3* gene is interrupted by an artificial intron (AI) that is removed from the *Ty1-H3mHIS3AI* mRNA intermediate by splicing, followed by reverse transcription and Ty1-IN mediated integration of Ty1*HIS3 denovo* into the genome or by homologous recombination with a pre-existing chromosomal Ty1 element or solo LTR (50). The 19 strains tested here carry ts mutations or deletions of Nups that are representative of NPC substructures (Figure 1A). Of the 19 strains tested, 9 were significantly decreased and 2 were significantly increased for Ty1 mobility (Figure 1B and Table 1). Four of the 7 members of the Nup84 outer ring subcomplex were tested (*nup84Δ*, *nup120Δ*, *nup133Δ*, *sec13-1*) and of these, *nup120Δ* and *sec13-1* strains had a ∼3.5-fold increase and ∼8.2-fold decrease in Ty1 mobility respectively (Figure 1B and Table 1). We tested five of the six members of the Nup170 inner ring subcomplex of which 4 (*nup170Δ, nup188Δ, nup53Δ, nup192–15*) had significantly decreased Ty1 mobility (Figure 1B and Table 1). The transmembrane ring subunit, Pom34, and the Nup159 cytoplasmic filamentous Nup are both required for wild type levels of Ty1 mobility with a 4-fold reduction in the *pom34Δ* mutant and a 50-fold reduction in the *nup159-1* mutant (Figure 1B and Table 1). Three of the nuclear basket deletion strains tested had a significant difference in Ty1 mobility compared to wild type with the *mlp1Δ* and *nup60Δ* strain each reduced by ∼3-fold and the *mlp2Δ* strain increased by ∼2.3-fold (Figure 1B and Table 1). Although Nup2 is not a core member of the NPC we included it in our study as a nuclear basket Nup (Figure 1A) because Nup2 is a mobile Nup that binds both the cytoplasmic and nuclear faces of the pore, interacts with Nup60, and has a role in chromatin organization and tRNA transcription (20,21,25,58,59). However, we did not detect a significant change in Ty1 mobility in the *nup2Δ* strain compared to the wild type strain (Figure 1B and Table 1).

The Ty1 mobility assay monitors Ty1 insertion into the genome mediated by Ty1-IN but also by homologous recombination with a pre-existing genomic Ty1 element or LTRs (60). To assess the frequency of Ty1 insertion mediated via IN versus homologous recombination, we transformed a wild type strain with a plasmid expressing wild type Ty1-IN [*Ty1-H3mHIS3AI* plasmid (pBDG633)] or a *Ty1-H3mHIS3AI* plasmid coding for a catalytically inactive Ty1-IN enzyme (pBDG924). We carried out the quantification assay with both plasmids and found that circa 35% of Ty1 mobility in the wild type strain can be attributed to homologous recombination (Supplementary Figure S1). Indeed, we demonstrate below that mutants with significant

Table 1. Summary of Ty1 replication data for NPC mutant yeast strains

NPC substructure	Yeast strain	Ty1 mobility frequency (SD)	Ty1 mobility ratio[a]	*SUF16*[b]	*SUP61*[b]	Ty1 mRNA[c]	Ty1 Gag protein levels[d]	Ty1 cDNA[e]	tLEU[f]	tLEU (denovo)[f]	tGLY[f]
–	wild type	6.80E−06 (3E−06)	1.0	1.0	1.0	1.0	1.0	1.2	1.0	1.0	1.0
Outer ring	*nup84Δ*	5.37E−06 (2E−06)	0.79	0.5	0.09	–	–	–	–	–	–
	nup120Δ	2.40E−05 (1E−05)	3.53	9.8	2.4	1.6	1.1	8.3	0.7	0.7	0.8
	nup133Δ	4.17E−06 (1E−06)	0.61	0.7	1.6	–	–	–	–	–	–
	sec13-1	8.28E−07 (3E−07)	0.12	0.05	0.07	1.2	0.84	0.4	1.0	0.8	0.7
Inner ring	*nup170Δ*	4.00E−07 (3E−07)	0.06	0.19	0.0	1.1	0.53	0.6	0.5	0.6	0.6
	nup188Δ	6.22E−07 (9.9E−07)	0.09	0.07	0.02	2.2	0.4	2.1	0.5	0.6	0.7
	nup53Δ	2.34E−06 (7E−07)	0.34	0.08	0.09	1.2	1.1	2.9	0.7	0.9	0.7
	nup59Δ	5.26E−06 (5E−06)	0.77	0.21	0.16	–	–	–	–	–	–
	nup192-15	5.44E−07 (3E−07)	0.08	0.0	0.09	2.2	0.73	1.0	1.1	0.9	1.2
Cytoplasmic	*nup159-1*	1.12E−07 (5E−08)	0.02	0.05	0.003	0.52	0.37	0.5	1.0	1.2	1.4
	nup42Δ	8.09E−06 (2E−06)	1.19	0.02	0.04	–	–	–	–	–	–
Transmembrane ring	*ndc1–4*	6.23E−06 (3E−06)	0.92	0.04	0.3	–	–	–	–	–	–
	pom34Δ	1.70E−06 (1E−06)	0.25	0.0	0.06	1.5	1.2	1.3	0.9	1.7	1.6
	pom152Δ	4.89E−06 (2E−06)	0.72	0.21	0.27	–	–	–	–	–	–
Central FG	*nup100Δ*	4.55E−06 (2E−06)	0.67	0.16	0.07	–	–	–	–	–	–
Nuclear	*nup2Δ*	8.07E−06 (6E−06)	1.19	0.21	0.25	1.6	–	–	0.51	0.44	0.62
	nup60Δ	2.18E−06 (2E−06)	0.32	0.0	0.03	0.19	0.23	0.2	0.5	0.6	0.5
	mlp1Δ	2.34E−06 (2E−06)	0.34	0.83	0.2	0.79	0.77	0.5	0.5	0.6	0.8
	mlp2Δ	1.53E−05 (1E−05)	2.25	2.1	0.63	1.3	0.75	1.1	0.6	0.6	0.8
	nup1Δ	6.84E−06 (5E−06)	1.0	0.12	–	1.65	0.81	–	0.4	0.78	0.91

[a]Compared to wild type Ty1 mobility.
[b]Compared to wild type Ty1 insertion upstream of the *SUF16* or *SUP61* loci.
[c]Compared to wild type Ty1 mRNA levels with *TAF10* as an internal control.
[d]Compared to wild type Ty1 Gag protein levels normalized to a GAPDH loading control.
[e]Compared to ratio of Ty1 cDNA to an endogenous Ty1 element.
[f]Compared to wild type tRNA levels with *TAF10* as an internal control.
Standard deviation (SD), experiments not done indicated with a dash.

reductions in Ty1 mobility display severe reductions in Ty1 targeting upstream of tRNA genes which is Ty1-IN mediated (Figures 4 and 5).

Nup60 is required for optimal Ty1 mRNA, Gag and tRNA levels

NPCs are bidirectional transporters that interact with cellular cargo entering and exiting the nucleus. Therefore, NPC mutants may restrict Ty1 transposition at various stages of the Ty1 life cycle such as transcription of the Ty1 element, export of processed Ty1 mRNA transcripts, reverse transcription of the Ty1 mRNA to cDNA, import of Ty1-IN into the nucleus and/or Ty1 cDNA integration into the genome. To determine if the significant differences in quantitative Ty1 mobility in NPC mutant strains were due to defects in Ty1 mRNA transcription and/or export we measured endogenous levels of Ty1 mRNA by quantitative real-time PCR (qPCR) and Ty1 Gag protein [processed (p49) and unprocessed (p45)] by quantitative western blot analysis in all NPC mutants with significant changes in Ty1 mobility.

To assess Ty1 mRNA expression in Nup mutant strains, cells were grown at 20°C to logarithmic phase, mRNA extracted, converted to cDNA and qPCR analysis performed. The *spt3Δ* mutant was used as a negative control as Spt3 is required for transcription of Ty1 elements (61). Of the 11 mutants with altered Ty1 mobility, the *nup60Δ* strain had the most dramatic reduction in Ty1 mRNA, generating only 19% of wild type Ty1 mRNA levels, suggesting that Nup60, which is located on the nuclear face of the yeast NPC, is required for expression of Ty1 elements (Figure 2A and Table 1). Interestingly, Nup60 interacts with tRNA genes but NPC contact is not specifically required for the binding of Pol III to tRNA genes or tRNA gene expression (21). Two other nuclear basket mutants, *mlp1Δ* and *mlp2Δ* expressed Ty1 mRNA at ∼79% and 133% of wild type levels, respectively and Ty1 Gag at 77% and 75% of wild type levels, respectively (Figure 2 and Table 1). The only other Nup mutant with reduced Ty1 mRNA levels was *nup159–1*, which is located on the cytoplasmic side of the NPC, and expressed Ty1 mRNA at 52% of wild type levels (Figures 1A and 2A). All other NPC mutants had Ty1 mRNA levels similar to or higher than the wild type strain (Figure 2A and Table 1).

Because all Ty1 polypeptides are generated from the same Ty1 mRNA, monitoring Ty1 Gag protein levels is a proxy for nuclear export of Ty1 element mRNA and also convenient as Ty1 Gag is the only Ty1 protein that can be detected at endogenous levels. We generated cell lysates from wild type and Nup mutant logarithmically growing cells and performed quantitative immunoblot analysis with anti-Ty1 Gag antibodies to assess Ty1-Gag protein levels and anti-GAPDH antibodies as a loading control (Figure 2B). The *spt3Δ* strain was used as a negative control as described above. As expected from the reduction in Ty1 mRNA expression, the *nup159–1* and *nup60Δ* mutants displayed reduced Ty1 Gag protein at 37% and 23% of wild type levels, respectively (Figure 2B and Table 1). Not predicted by the Ty1 mRNA expression data, however, was the reduction in Ty1 Gag levels detected in a subset of mutants from the Nup170 inner ring sub-complex. The *nup170Δ*, *nup188Δ* and *nup192–15* mutants had 53%, 40% and 73% of wild type Ty1 Gag levels, respectively (Figure 2B, Table 1). Therefore, the Nup170 inner ring subcomplex may have a role in export of Ty1 mRNA into the cytoplasm. The remainder of the Nup mutants displayed 75% or higher levels of Ty1 Gag when compared to wild type suggesting that mRNA export and translation of Ty1 transcripts is not dramatically altered (Figure 2B and Table 1).

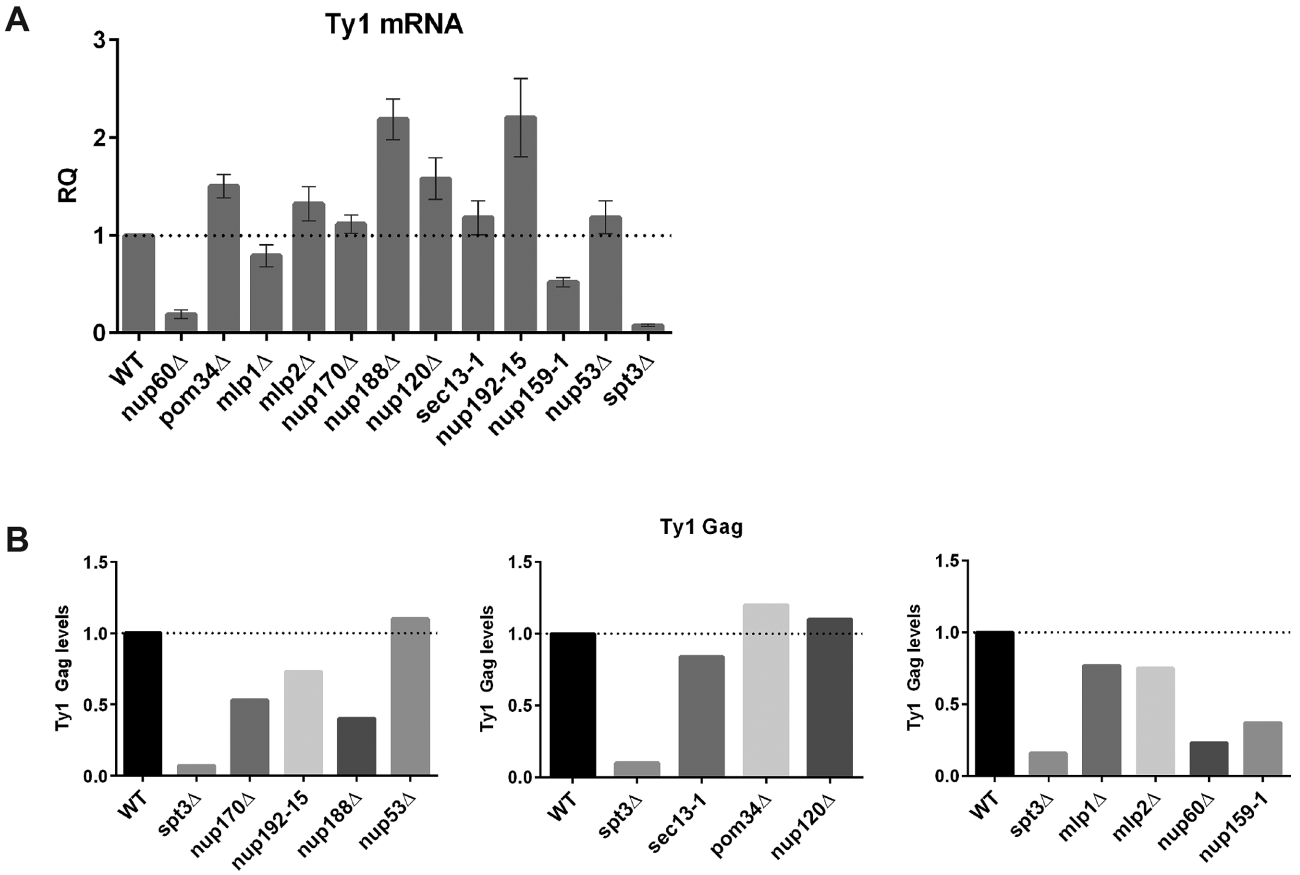

Figure 2. Nup60 is required for Ty1 mRNA expression and Ty1 Gag production. (**A**) qPCR analysis of Ty1 mRNA was performed in triplicate on the following mutant yeast strains: wild type (WT), *nup60Δ, pom34Δ, mlp1Δ, mlp2Δ, nup170Δ, nup188Δ, nup120Δ, sec13–1, nup192-15, nup159-1* and *nup53Δ*. *spt3Δ* serves as a negative control. Strains were grown at 20°C to log phase for RNA extractions. The bar graph shows relative quantification (RQ) of Ty1 transcript compared to a control (*TAF10*) and relative to wild type Ty1 mRNA set to 1. (**B**) Ty1 Gag protein levels were analyzed in the same strains as (A), grown at 20°C to log phase. Anti-Gag sera was used to detect unprocessed (p49) and processed (p45) Gag levels by quantitative western blot with fluorescently labeled secondary antibodies. Ty1 Gag fluorescence signals (p49 and p45) were normalized to GAPDH, averaged, quantified using Image Studio software and are reported relative to wild type.

Active Pol III transcription is thought to be required for Ty1 insertion. A point mutation in box B of the *SUF16* tRNA promoter that dramatically reduces transcription also reduces Ty1 element insertion (6). Also, Ty1 does not target to the tRNA relic gene *ZOD1* which has very low transcription levels (62,63). To determine if Pol III transcription is affected in our panel of NPC mutants, we measured the level of leucine (*tLEU* and unprocessed *tLEU* called *tLEU denovo*) and glycine tRNA transcripts (*tGLY*) by qPCR in cells grown to log phase at 20°C. We found that *tLEU* and *tLEU denovo* transcript levels were reduced by ∼50% in *nup60Δ*, *mlp1Δ*, *nup170Δ* and *nup188Δ* strains (Figures 3A, 3B and Table 1). Notably, the *nup60Δ* mutant also had a ∼50% reduction in *tGLY* levels whereas all other NPC mutants expressed *tGLY* at 60% of wild type levels or higher (Figure 3C and Table 1). Our tRNA expression data suggests that a 2-fold reduction in Ty1 genomic insertion in NPC mutants may be attributed to a reduction in Pol III transcription. However, any further reduction in Ty1 targeting in NPC mutants may be due to a defect in the integration process.

Ty1 cDNA levels are affected in only a subset of Nup mutant strains

One of the limiting steps in the Ty1 life-cycle is the reverse-transcription of the Ty1 mRNA to cDNA (5). It has previously been shown that deletion of *NUP120* or *NUP133* results in increased Ty1 cDNA and deletion of *NUP84*, *NUP120* or *NUP133* also causes an increase in Ty3 cDNA levels (27,29,32). One interpretation of this data is that the Ty1 cDNA increase is due to accumulation of the cDNA in the cytoplasm in the absence of efficient nuclear transport (27). Another interpretation is that PIC nuclear entry is enhanced upon disruption of the Nup84 outer ring subcomplex (32). We analyzed endogenous Ty1 cDNA levels in wild type and Nup mutants with altered Ty1 mobility by Southern blot analysis of yeast genomic DNA digested with PvuII, which liberates a ∼2 kb fragment of Ty1 cDNA, and hybridization of a probe containing a 1517 bp C-terminal fragment of the endogenous Ty1 element. We used software to quantify the ratio of Ty1 cDNA compared to a Ty1 element fragment (Ty1 control). Of the 11 Nup mutant strains we tested, 3 (*mlp2Δ, nup192-15, pom34Δ*) had a wild type ratio of Ty1 cDNA to Ty1 control and 3 (*nup53Δ, nup120Δ,*

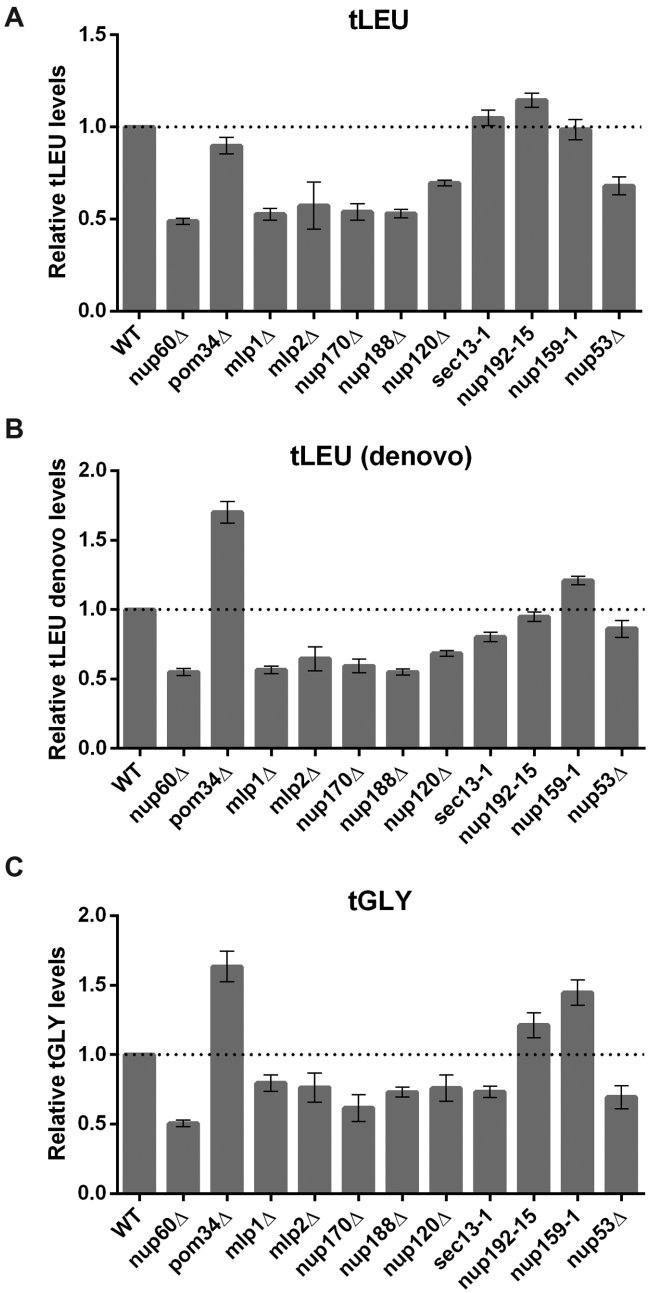

Figure 3. tRNA levels are reduced in a subset of NPC mutant strains. qPCR analysis was used to measure (**A**) *tLEU*, (**B**) *tLEU denovo* and (**C**) *tGLY* levels in wild type (WT), *nup60Δ, pom34Δ, mlp1Δ, mlp2Δ, nup170Δ, nup188Δ, nup120Δ, sec13-1, nup192-15, nup159-1* and *nup53Δ* strains. RNA was isolated from strains grown to log phase at 20°C and qPCR was performed in triplicate with *TAF10* expression used as an internal control. Mutant gene expression values are derived by comparing levels to wild type, which is set to 1.0.

nup188Δ) had increased ratios of Ty1 cDNA to Ty1 control compared to a wild type strain (Supplementary Figure S2 and Table 1). This data suggests Ty1 mobility defects in these mutants are not due to low Ty1 cDNA production. The *nup120Δ* strain, which has increased Ty1 mobility, had an ∼8-fold higher ratio of Ty1 cDNA to Ty1 control than the wild type strain (Supplementary Figure S2 and Table 1); which has been previously observed (29). The remainder of the Nup mutants had a 1.5- to 3-fold reduction in Ty1 cDNA ratios (*mlp1Δ*, *nup159-1*, *nup170Δ*, *sec13-1*) whereas the *nup60Δ* mutant had a 6-fold reduction in Ty1 cDNA levels compared to wild type, which is not surprising considering the defects in Ty1 mRNA synthesis and Ty1 protein levels in this mutant (Supplementary Figure S2, Figure 2 and Table 1). The reduced Ty1 cDNA levels in the *mlp1Δ*, *nup159-1*, *nup170Δ*, *sec13-1* mutants could be in part causing Ty1 mobility defects although the *nup170Δ* mutant has ∼60% of wild type Ty1 cDNA levels but a 17-fold reduction in transposition mobility (Figure 1B and Supplementary Figure S2, Table 1).

Ty1 IN can enter the nucleus of NPC mutant strains

To determine if the transposition defect observed in the NPC mutant strains was due to a Ty1-IN nuclear localization defect we analyzed Ty1-IN localization in the mutant strains by fluorescence microscopy. We constructed a Ty1-IN expression plasmid with a *PGK1* promoter and the fluorescent mCherry tag appended to the C-terminus of Ty1-IN. The constitutively expressed *PGK1* promoter is not among the list of genes with inducible promoters, such as the *GAL* genes, that have been shown to interact directly with NPCs (13,20), therefore Ty1-IN-mCherry expression should not be affected by the NPC mutation. NPC mutant strains carrying the Ty1-IN-mCherry plasmid were grown to log phase followed by nuclear staining and live cell fluorescence imaging. All of the eleven NPC mutants with altered Ty1 mobility demonstrated localization of Ty1-IN into the nucleus suggesting that none of these NPC components are critical for Ty1-IN nuclear entry (Supplementary Figure S3).

Ty1 insertion requires NPC subunits

Since all but one (*nup60Δ*) of the Nup mutants with low Ty1 mobility have relatively normal (*pom34Δ*) or higher (*nup53Δ, nup192–25)* Ty1 mRNA, Gag or cDNA levels or levels higher than predicted from the reduction in Ty1 mobility (*sec13-1, mlp1Δ, nup159-1, nup170Δ, nup188Δ*) in addition to proper Ty1-IN nuclear import, we hypothesized that the reduction in Ty1 mobility is due to an inability of the Ty1 element to insert into the genome. To test our hypothesis, we induced endogenous transposition of pre-existing chromosomal Ty1 elements by growing wild type and Nup mutant strains at 20°C for 3 days, isolating genomic DNA and analyzing Ty1 insertion events upstream of the *SUF16* glycine tRNA gene [tG(GCC)C] on chromosome III, which has previously been shown to be a transposition hotspot (64). The *SUF16* locus is located within the pericentromere of chromosome III which is a ∼50kb region to the left and right side of the centromere (65). tRNA genes have a role in the enrichment of condensin at pericentromeres, therefore we postulated that Ty1 element insertion upstream of tRNA genes in the pericentromere may have different requirements from Ty1 element insertion upstream of tRNA genes located on the chromosome arm (66). The serine tRNA gene *SUP61* [tS(CGA)C] is located outside the pericentromere on the arm of chromosome III. Interestingly, *SUP61* is recruited to and actively transcribed at

NPCs during M phase, evoking a potential role for the Nups in targeting Ty1 element insertion upstream of *SUP61* (21).

We designed a primer complementary to either the *SNR33* or *BUD31* locus on chromosome III adjacent to *SUF16* and *SUP61,* respectively. A second primer that hybridizes within the Ty1 element was used for both PCR assays. Each NPC mutant strain was assayed in triplicate with a *spt3Δ* strain used as a negative control for Ty1 replication. Quantification of Ty1 integration was achieved by software that calculated the total band intensity for each strain as described (54). PCR amplification of *CPR7* located on chromosome X was used as a control to ensure that PCR competent genomic DNA was present. Due to the position of the primers, periodic insertion of Ty1, is detected in a window of ∼750–1500 bp upstream of *SUF16* and *SUP61* in a ladder due to nucleosome positioning. Although Ty1 elements can insert in either orientation (62), this PCR assay only detects Ty1 elements inserted in the forward direction.

When compared to the wild type strain, Ty1 insertion upstream of both the *SUF16* and *SUP61* tRNA genes was almost negligible in the eight of the nine Nup mutant strains with reduced Ty1 mobility: *nup53Δ, nup60Δ, nup159–1, nup170Δ, nup188Δ, nup192–15, pom34Δ* and *sec13-1* (Figures 4, 5 and Table 1). Three NPC mutants had different Ty1 insertion frequencies depending on the locus tested. The *mlp1Δ* mutant, which had ∼3-fold reduced Ty1 mobility compared to wild type (Figure 1B and Table 1) had 0.83 Ty1 insertion frequency upstream of *SUF16* but only 0.2 Ty1 insertion frequency upstream of *SUP61* when compared to wild type (Figures 4A, 5A and Table 1). The *mlp2Δ* strain which had significantly increased Ty1 mobility (∼2.3-fold compared to wild type) had a 2.1-fold increased Ty1 insertion upstream of *SUF16* but 63% of wild type Ty1 insertion upstream of *SUP61* (Figures 4A, 5A and Table 1). In corroboration with the ∼3.5-fold increase in Ty1 mobility, the *nup120Δ strain* had increased Ty1 insertion upstream of both tRNA genes, however the increase was more pronounced upstream of *SUF16* (9.8-fold) compared to *SUP61* (2.4-fold) (Figures 1B, 4B, 5B and Table 1). As well, in 3 independent cultures, the majority of the *nup120Δ* Ty1 insertions occurred in one nucleosome position upstream of the *SUF16* gene but did not favour a particular nucleosome upstream of the *SUP61* gene (Figure 4B, asterisk, Figure 5B). The Ty1 insertion data suggests that a subset of Nups are absolutely required for Ty1 element insertion upstream of pericentromeric and chromosome arm tRNA genes, whereas the Mlp1 nuclear basket protein may be more important for insertion at tRNA genes located on chromosome arms. As well, the Mlp2 nuclear basket protein and the Nup120 outer ring protein are more inhibitory to Ty1 element insertion upstream of pericentromeric tRNA genes than chromosome arm tRNA genes.

Mlp1 interacts with the Nuclear abundant poly(A) RNA-binding protein 2 (Nab2) which is an essential protein involved in mRNA poly(A) tail length control, messenger ribonucleoprotein particle (mRNP) formation, and nuclear mRNP export (67–71)**.** Interestingly, Nab2 also occupies all RNA Pol III transcribed genes and therefore may have a role in Ty1 transposition (72). We tested a set of *NAB2* mutants that eliminate the Mlp1-Nab2 interaction (71) for defects in Ty1 insertion at *tGLY* but found that all of the *NAB2* mutants had *tGLY* Ty1 insertion levels that were comparable to wild type (Supplementary Figure S4). We also analyzed Ty1 *tGLY* insertion levels in a *nab2–34* essential ts mutant (72). Although the conditions we used allow for Ty1 transposition in the S288C strain background, in the *nab2–34* isogenic wild type strain (W303) very little Ty1 insertion was detected (Supplementary Figure S4C). However, we detected a 6-fold increase in Ty1 insertion in the *nab2–34* mutant suggesting that Nab2 may be inhibitory to Ty1 transposition in the W303 background (Supplementary Figure S4C).

Ty1 is mistargeted in the absence of Nup proteins

The *HIS3* marked Ty1 element mobility assay (Figure 1) cannot distinguish between targeting of Ty1 elements upstream of Pol III-transcribed genes and mis-targeting of Ty1 elements into the genome and only depends on insertion into a locus that does not impede *HIS3* gene expression. Therefore, we assessed Ty1 insertion in Nup deletion strains that had wild type levels of Ty1 mobility (*nup84Δ, nup133Δ, nup59Δ, nup42Δ, ndc1–4, pom152Δ, nup100Δ* and *nup2Δ,* Figure 1B). We first analyzed insertion upstream of *SUF16* and, surprisingly, noticed that all Nup mutants with wild type Ty1 mobility were impaired for Ty1 insertion upstream of the *SUF16* locus (Figure 6). Deletion of *NUP84* and *NUP133*, both members of the Nup84 outer ring subcomplex, caused Ty1 insertion at *SUF16* to diminish by 50% and 30%, respectively (Figure 6A and Table 1). In addition, Ty1 insertion in the *nup133Δ* mutant appeared to favor the first insertion site (asterisk, Figure 6A) and one of the *nup84Δ* cultures had an extra insertion site not detected in the wild type strain (arrow, Figure 6A). Deletion of the Nup100 central FG-repeat Nup and Nup59 inner ring Nup, caused a ∼6-fold and ∼5-fold reduction, respectively, in Ty1 insertion upstream of *SUF16* compared to wild type (Figure 6B and Table 1). The *ndc1–4* and *pom152Δ* transmembrane Nup mutants had a ∼25-fold and ∼5-fold reduction, in Ty1 insertion upstream of *SUF16* compared to wild type (Figures 6A, 6B and Table 1). Deletion of the cytoplasmic FG Nup, Nup42, had the most severe effect on Ty1 insertion with a ∼50-fold reduction (Figure 6A and Table 1). We observed similar results upon testing Ty1 targeting upstream of the *SUP61* serine tRNA gene (Figure 7). There were two notable exceptions - *nup133Δ* had a 1.6-fold increase (compared to a 30% reduction for *SUF16*) and *nup84Δ* had a 11-fold decrease (compared to a 2-fold decrease for *SUF16*) in *SUP61* targeting when compared to wild type (Figure 7A and Table 1).

Removing two of the nuclear basket Nups did not affect Ty1 mobility but did impact the efficiency of Ty1 targeting upstream of tRNA genes. Deletion of Nup2, a mobile Nup that is known to interact with chromatin and tRNA genes (21,25,58,59), resulted in wild type Ty1 mobility but reduced Ty1 targeting upstream of *SUF16* to 21% of wild type levels (Figure 6C and Table 1). Deletion of Nup2 also reduced Ty1 targeting upstream of the *SUP61* gene ∼4-fold compared to wild type Ty1 levels (Figure 7C and Table 1). A similar result was found when Ty1 targeting was analyzed in a *nup2Δ* mutant using a primer that hybridizes to all 16 *tGLY* genes (Supplementary Figure S5A). Removal of the

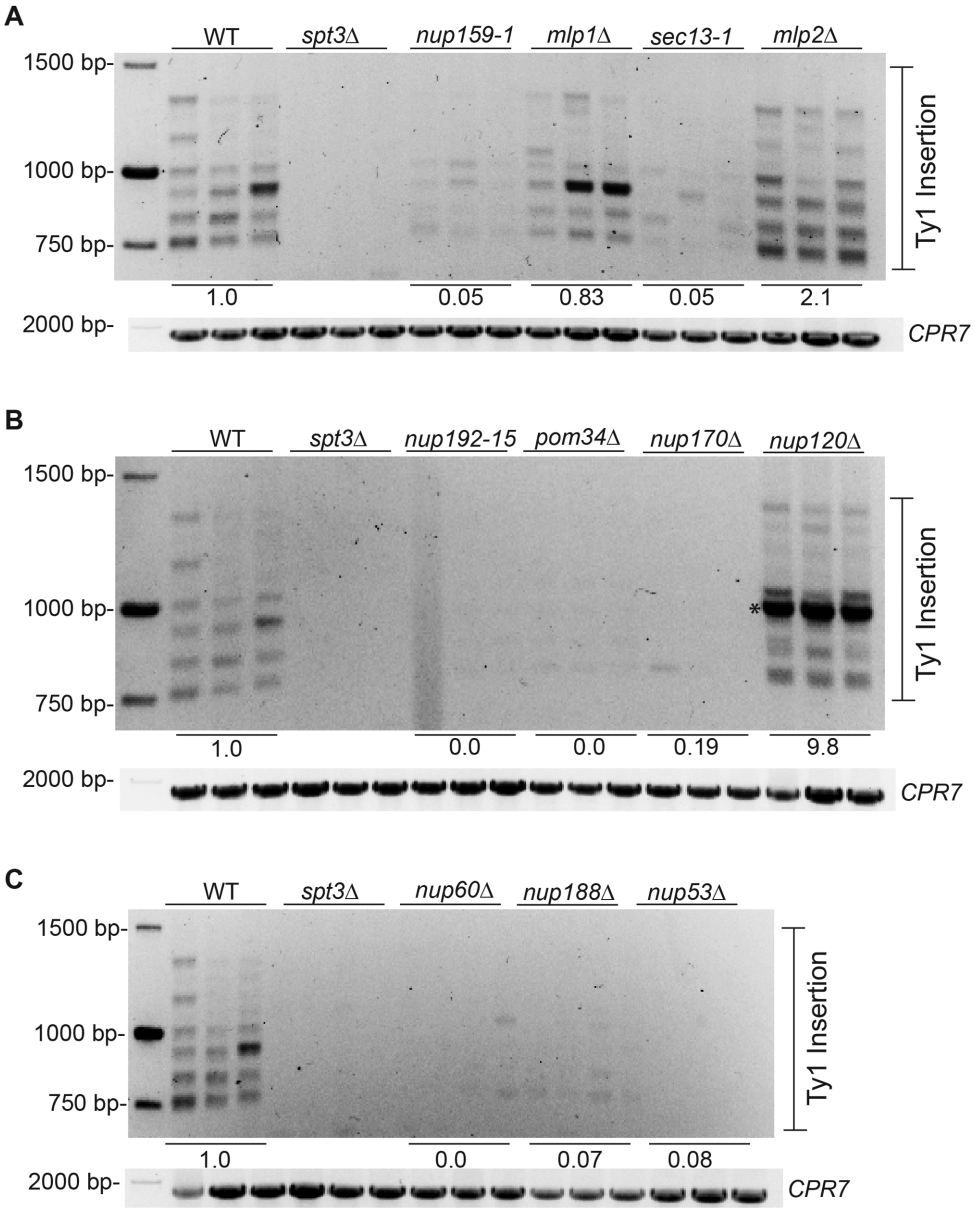

Figure 4. Ty1 insertion upstream of the *SUF16* tRNA hotspot is severely impaired in multiple NPC mutant strains. The indicated strains (**A**) wild type (WT), *spt3Δ*, *nup159-1 mlp1Δ*, *sec13-1*, *mlp2Δ* (**B**) WT, *spt3Δ*, *nup192-15*, *pom34Δ*, *nup170Δ*, *nup120Δ* and (**C**) WT, *spt3Δ*, *nup60Δ*, *nup188Δ*, *nup53Δ* were each grown in triplicate for 3 days at 20°C. Genomic DNA was extracted, then used for PCR analysis with one primer located in the Ty1 element and the other located adjacent to the *SUF16* locus. Ty1 insertion events are represented by a ladder of bands coincident with nucleosome positioning. The lower panel is a control PCR of the *CPR7* locus to demonstrate the presence of PCR-competent genomic DNA in each sample. Image Lab software was used to quantitate the intensity of Ty1 insertion events in each lane, averaged for each yeast strain and compared to wild type which was set to a level of 1.0. An asterisk (*) denotes a preferred Ty1 element insertion site in the *nup120Δ* strain.

Nup1 nuclear basket protein, which is required for mRNA export (73,74), did not alter Ty1 mobility (Figure 8A) but resulted in an 8.3-fold decrease in Ty1 insertion upstream of *tGLY* genes (Figure 8B). The *nup1Δ* mutant produced 1.65-fold more Ty1 mRNA than wild type and produced Ty1 Gag at 81% of wild type which is consistent with the fact that Ty1 mobility in the *nup1Δ* strain is similar to wild type (Figures 8C, 8D). The *nup1Δ* mutant had a 60% reduction in *tLEU* levels compared to wild type but expressed *tLEU denovo* and *tGLY* at levels similar to wild type (Figure 8E). It has been previously determined that *nup1Δ* strains do not accumulate unspliced tRNAs suggesting that *tLEU denovo* should be exported into the cytoplasm for splicing at the mitochondrial outer surface (75,76). Therefore, the low *tLEU* levels in the *nup1Δ* strain may reflect defects in another aspect of tRNA maturation or stability. The fact that Ty1 mobility is similar to wild type levels in both the *nup1Δ* and *nup2Δ* nuclear basket mutants, yet Ty1 element targeting is impaired, suggests that Ty1 elements may be mistargeted to alternative loci.

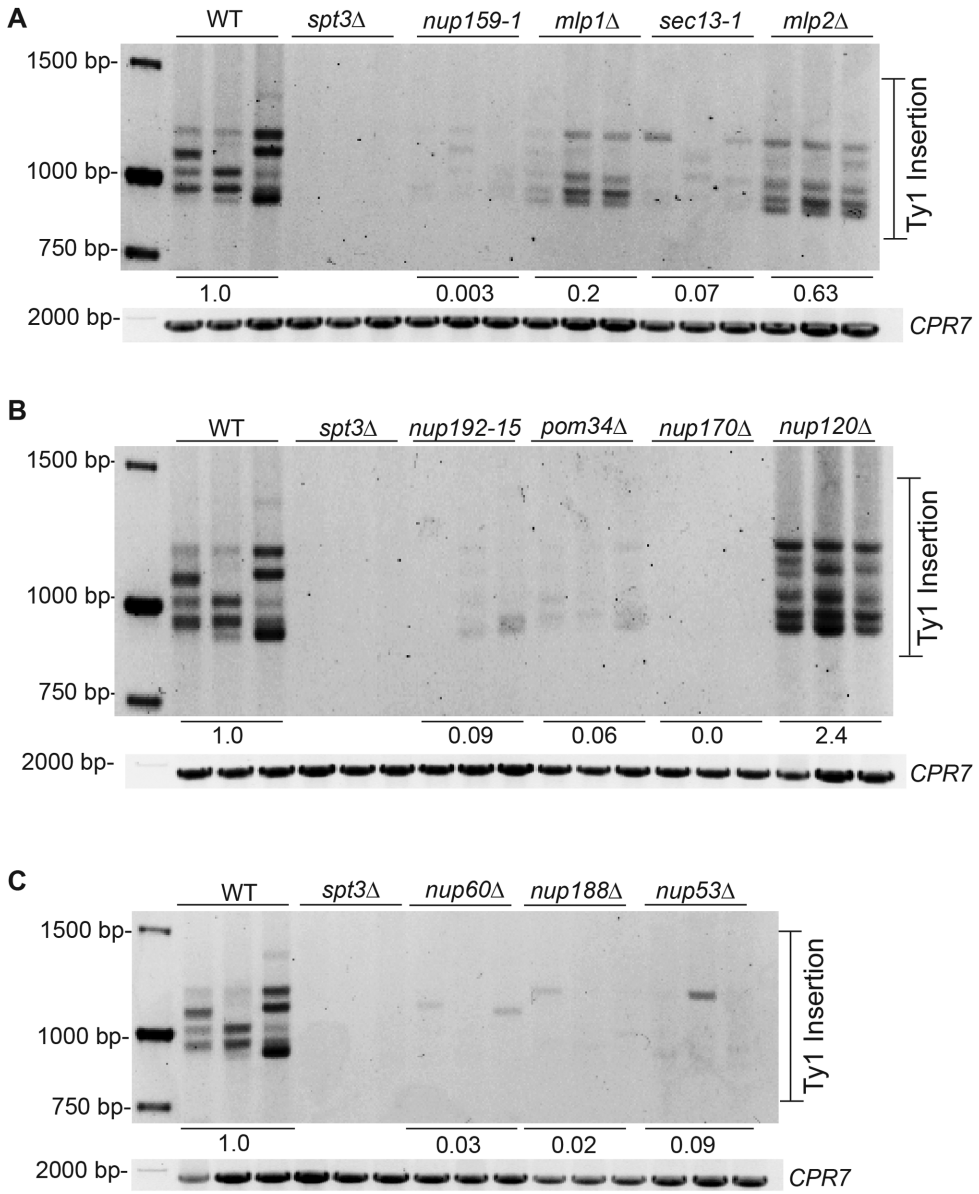

Figure 5. Ty1 insertion upstream of the *SUP61* tRNA arm locus is dependent on the NPC. The indicated strains (**A**) wild type (WT), *spt3Δ*, *nup159-1 mlp1Δ*, *sec13-1*, *mlp2Δ*, (**B**) WT, *spt3Δ*, *nup192–15*, *pom34Δ*, *nup170Δ*, *nup120Δ* and (**C**) WT, *spt3Δ*, *nup60Δ*, *nup188Δ*, *nup53Δ* were each grown in triplicate for 3 days at 20°C. Genomic DNA was extracted, then used for PCR analysis with one primer located in the Ty1 element and the other located adjacent to the *SUP61* locus. The range of Ty1 insertion events is marked to the right of each gel. The lower panel is a control PCR for the *CPR7* locus to demonstrate the presence of genomic DNA in each sample. Image Lab software was used to quantitate the intensity of Ty1 insertion events in each lane, averaged for each yeast strain and compared to WT set to a level of 1.0.

NPC membrane curvature by Nup1 and Nup60 plays a role in Ty1 insertion

Given that the NPC's nuclear basket substructure (Nup1-Nup2-Nup60-Mlp1-Mlp2) is located on the nuclear side of the NPC and has been strongly linked to genomic processes such as chromatin organization, transcription, mRNA export and tRNA gene expression (24,77,78) we chose to focus on these Nups and protein complexes that interact with the nuclear basket, for further study. Thus far, our studies indicate that the nuclear basket has a role in Ty1 element insertion into the genome, however we employed complete gene deletions which remove all protein function and therefore have pleiotropic phenotypes. To assess nuclear basket mutants that retain partial activity we acquired Nup mutants that retained some activity but removed specific protein domains, to test the impact of the mutation on Ty1 element insertion.

It has recently been discovered that Nup1 contains an AH and an adjacent α-HR (Figure 9A) that are required for NE membrane curvature at the NPC insertion site and anchoring the nuclear basket to the NPC, respectively (46). We tested for Ty1 insertion defects in yeast strains carrying Nup1 lacking the AH (nup1Δ1–32) or HR (nup1Δ85–123) domains which results in partial mislocalization of Nup1

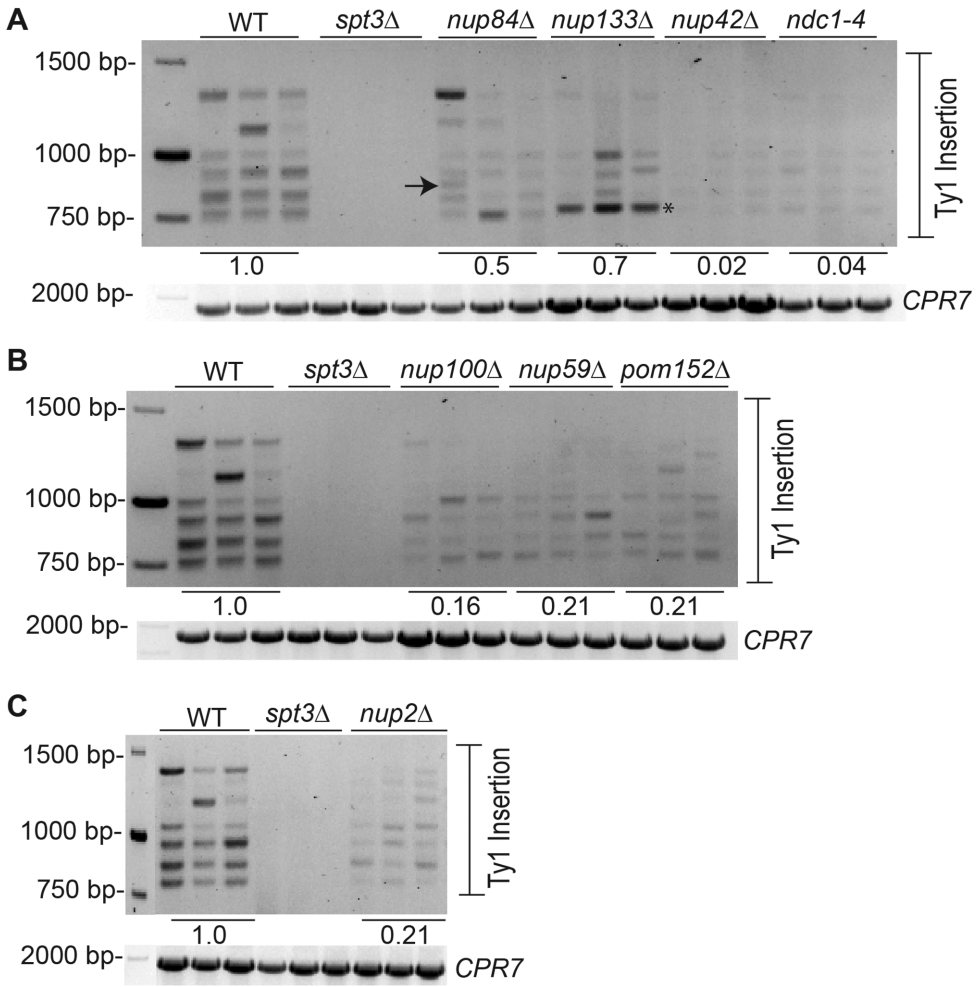

Figure 6. NPC mutants with wild type Ty1 mobility have defects in Ty1 insertion upstream of the *SUF16* hotpot locus. The following strains with wild type Ty1 mobility: (**A**) wild type (WT), *nup84Δ*, *nup133Δ*, *nup42Δ*, *ndc1–4,* (**B**) WT, *nup100Δ, nup59Δ, pom152Δ* and (**C**) WT, *nup2Δ* were grown for 3 days at 20°C in triplicate. *spt3Δ* serves as a negative control. Genomic DNA was extracted then used for PCR analysis with a Ty1 primer and a primer adjacent to *SUF16*. The *CPR7* panel is a control PCR to demonstrate the presence of genomic DNA in each sample. Image Lab software was used to quantitate the intensity of Ty1 insertion events in each lane, averaged for each yeast strain and compared to WT set to a level of 1.0. An arrow (→) denotes a novel insertion site in the *nup84Δ* strain and an asterisk (*) denotes a preferred insertion site in the *nup133Δ* strain.

into the nucleoplasm (46). Both mutants had higher Ty1 insertion levels than a wild type strain - nup1Δ1–32 had ∼11-fold higher and nup1Δ85–123 had ∼1.8-fold higher when compared to a wild type strain (Figure 9B). Not only is Ty1 inserted more frequently but there is a strong bias in the Ty1 element insertion position with the second nucleosome primarily targeted in the nup1Δ1–32 mutant and a single site targeted in the nup1Δ85–123 mutant ∼five nucleosomes upstream of the tRNA gene (Figure 9B). Both mutants had no impairment in Ty1 mRNA or Gag levels and the nup1Δ1–32 mutant had wild type tRNA levels whereas the nup1Δ85–123 mutant expressed tRNA genes at ∼61–69% of wild type levels (Figure 9C–E). The reduction in tRNA gene expression does not appear to affect overall Ty1 insertion frequency.

Nup60, similar to Nup1, has AH and HR regions (Figure 10A) implicated in membrane curvature and nuclear basket tethering, respectively (46). Removal of the Nup60 AH (nup60Δ1–47) or HR (nup60Δ48–162) domains results in partial detachment of Nup60 from the nuclear basket (46). Removal of both AH and HR domains (nup60Δ1–162) causes the majority of Nup60 to mislocalize to the nucleoplasm and abnormal clustering of Mlp1 and Mlp2 (46). Since the *nup60Δ* mutant is required for Ty1 mRNA expression (Figure 2A), we first tested Ty1 mRNA levels in the Nup60 AH and HR mutants. All of the Nup60 AH and HR mutants expressed Ty1 mRNA at wild type levels suggesting either that sufficient Nup60 remains attached to the nuclear basket to allow Ty1 mRNA expression or that the role of Nup60 in Ty1 expression does not require tethering to the NPC (Figure 10C). Likewise, Ty1 Gag was expressed at 64% of wild type, or above wild type levels and tRNA gene expression was not affected in the Nup60 AH and HR mutants (Figures 10D and 10E). We tested Ty1 insertion upstream of *tGLY* genes in the Nup60 AH and HR mutants and noticed a change of Ty1 insertion pattern in each mutant suggesting that either nucleosome positioning or Ty1 targeting is affected in these mutants (Fig-

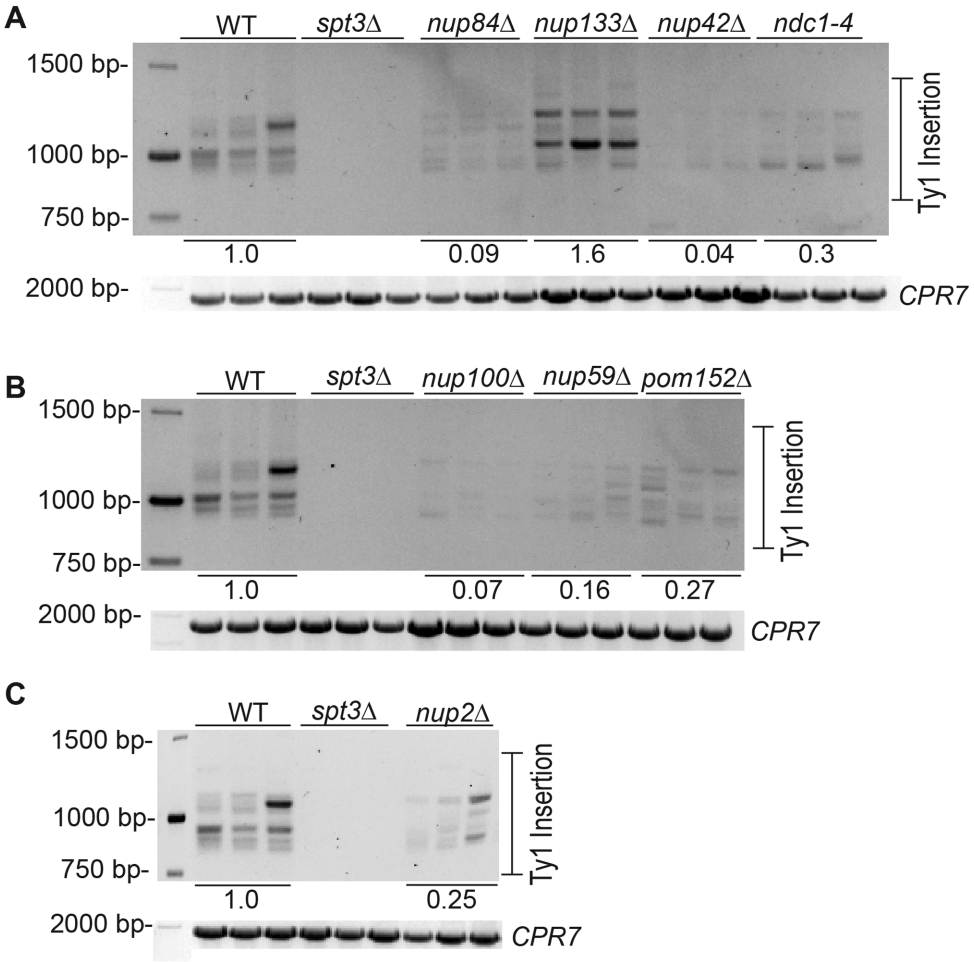

Figure 7. NPC mutants with wild type Ty1 mobility have defects targeting Ty1 elements upstream of the *SUP61* tRNA arm locus. The following strains with wild type Ty1 mobility: (**A**) wild type (WT), *nup84Δ*, *nup133Δ*, *nup42Δ*, *ndc1–4,* (**B**) WT, *nup100Δ, nup59Δ, pom152Δ* and (**C**) WT, *nup2Δ* were grown for 3 days at 20°C in triplicate. *spt3Δ* as a negative control. Genomic DNA was extracted, then used for PCR analysis with a Ty1 primer and a primer adjacent to *SUP61*. The lower panel is a control PCR of the *CPR7* locus to demonstrate that genomic DNA is present in each sample. Image Lab software was used to quantitate the intensity of Ty1 insertion events in each lane, averaged for each yeast strain and compared to WT set to a level of 1.0.

ure 10B). The insertion frequency was reduced to 61% and 47% of wild type in the nup60Δ1–47 and nup60Δ48–162 mutant, respectively, whereas the nup60Δ1–162 mutant had wild type Ty1 insertion levels (Figure 10B). Therefore, the restoration of Ty1 mRNA and Ty1 Gag levels, compared to the *nup60Δ* mutant, allows Ty1 element insertion upstream of *tGLY* genes but the nucleosome targeting is altered when the interaction between Nup60, the inner nuclear membrane and the nuclear basket is deficient.

Monoubiquitylation of Nup60, at one of 8 lysines between Lys105 and Lys175 (Figure 11A), controls the dynamics of Nup60 association with the NPC and contributes to the DNA-damage response and telomere repair (79,80). Some of the Nup60 ubiquitylated lysine residues are in the Nup60 HR region that impact Ty1 targeting (Figures 10A and 11A). To characterize the role of Nup60 ubiquitylation on Ty1 targeting we utilized a Nup60 ubiquitin (Ub) deficient mutant [nup60-K(105–175)R] that can no longer be conjugated to Ub (80). In the nup60-K(105–175)R mutant, the efficiency of Ty1 insertion upstream of *tGLY* genes was ∼58% that of a wild type strain, however, unlike the Nup60 HR mutant, the targeting pattern was similar to wild type (Figure 11B). The nup60-K(105–175)R Ub mutant has a 35% increase in Ty1 mRNA compared to wild type but a 26% reduction in Ty1 Gag protein levels compared to wild type (Figures 11C and 11D). Genotoxic stress, which prompts Nup60 ubiquitylation (80), may change the role of Nup60 in Ty1 replication, especially since the nup60-K(105–175)R mutant has an increase of unrepaired DNA lesions (80). However, since ubiquitylated Nup60 preferentially interacts with Nup84-Nup133, the 42% reduction of Ty1 insertion in a Nup60 Ub mutant could be due to an impaired interaction with the Nup84 outer ring subcomplex or indirect effects due to changes to the NPC structure (80).

Nup60 contains 2 SUMOylation sites: Lys440,442 and Lys505 (Figure 11A), however the function of Nup60 SUMOylation is not yet known (80). We studied the role of Nup60 SUMOylation with a Nup60 yeast strain containing a triple SUMO site mutation [Nup60-K(440–42, 505)R] integrated into the genome. The Nup60-K(440–42, 505)R mutant, which cannot be SUMOylated, had a ∼3-fold reduction in Ty1 insertion compared to wild type (Figure 11B).

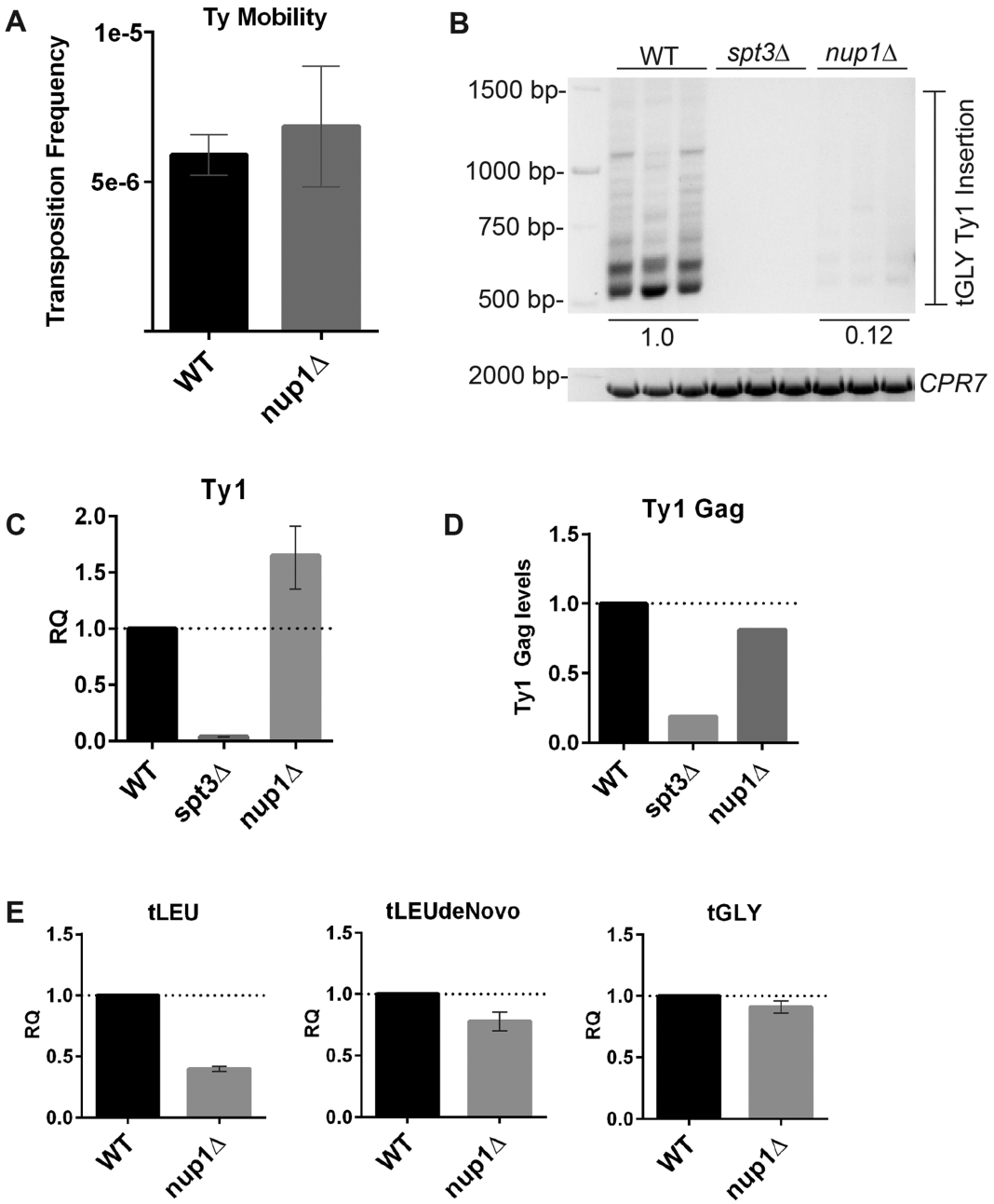

Figure 8. Nup1 is required for Ty1 insertion upstream of *tGLY* genes. (**A**) Ty1 mobility measured in a *nup1Δ* yeast strain compared to wild type (WT). Yeast strains carrying a Ty1-HIS3AI plasmid were grown for 5 days at 20°C in SC-URA media after which cells were plated on SC-URA and SC-URA-HIS plates and grown for 2 days at 25°C. Colonies were counted to calculate transposition frequency of each strain. (**B**) Genomic DNA was extracted from WT, *nup1Δ*, and *spt3Δ* yeast strains grown in YPD media for 3 days at 20°C in triplicate. Ty1 insertions upstream of *tGLY* tRNA genes (GCC; 16 copies) were amplified by PCR and quantified relative to WT. (**C**) Relative quantification (RQ) of Ty1 mRNA levels in *spt3Δ* and *nup1Δ* strains normalized to an internal *TAF10* control and compared to wild type which was set to 1. (**D**) Bar graphs generated from quantitative immune blots monitoring Ty1 Gag (p49 and p45) protein levels relative to GAPDH used as a loading control in WT, *spt3Δ* and *nup1Δ* strains. (**E**) *tLEU*, *tLEU denovo* and *tGLY* tRNA levels in logarithmically growing WT and *nup1Δ* strains. tRNA levels were normalized to *TAF10* and compared to wild type tRNA levels which were set to 1.

Importantly, the Nup60-K(440–42, 505)R SUMO mutant expressed Ty1 mRNA (92%), Ty1 Gag (83%) and tRNA genes at levels similar to wild type (Figure 11C–E). The Siz1 and Siz2 SUMO ligases are responsible for SUMOylation of Nup60 and the Ulp1 SUMO protease is responsible for removing the Nup60 SUMOylation (80). To determine the importance of SUMOylation on Ty1 targeting we analyzed Ty1 insertion upstream of *tGLY* genes in *siz1Δ*, *siz2Δ*, and *ulp1–333* mutant strains. We also included an *MMS21* mutant (*mms21–1*) because Mms21 is a SUMO E3 ligase that mediates the relocation of DNA double strand breaks to the nuclear periphery (81). Deleting Siz1 did not reduce Ty1 insertion upstream of *tGLY* while removing Siz2 caused a modest 32% decrease in Ty1 insertion upstream of *tGLY*

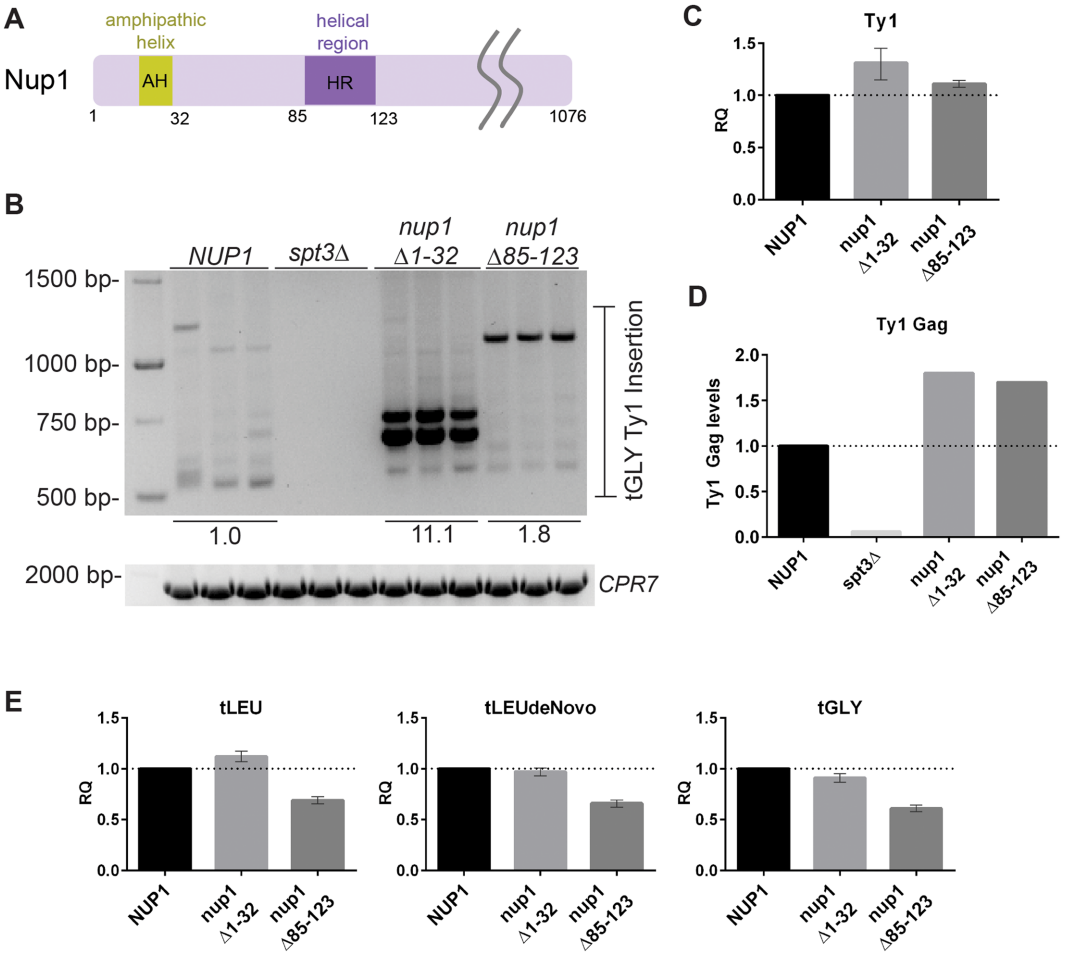

Figure 9. The Nup1 N-terminal AH and HR domains affect Ty1 element positioning upstream of *tGLY* loci. (**A**) Nup1 protein schematic with the AH and HR highlighted as in (46). (**B**) Ty1 insertion upstream of *tGLY* (GCC) loci for a *nup1Δ* yeast strain carrying a plasmid expressing either full-length nup1 (*NUP1*), nup1Δ1–32 or nup1Δ85–123 fused to mCherry. Ty1 insertion levels were quantified for each strain and normalized to wild type levels. The *spt3Δ* yeast strain is a negative control for Ty1 replication (**C**, **E**) Ty1 mRNA and tRNA (*tLEU*, *tLEU denovo*, *tGLY*) levels were measured by qPCR and normalized to *TAF10*. Relative quantification (RQ) values of mutant strains were compared to wild type which was set to 1. (**D**) Ty1 Gag (p49 and p45) protein levels measured with quantitative western blots and presented in a bar graph. Gag levels were quantified relative to GAPDH which was used as a loading control and normalized to wild type Gag/GAPDH.

as compared to wild type (Figure 11G). As well, the *ulp1–333* mutant had 82% of wild type Ty1 insertion upstream of *tGLY* (Figure 11F). However, the *mm21–1* mutant had a more dramatic phenotype with a reduction in Ty1 insertion of ∼3.7-fold compared to wild type (Figure 11F). It has not yet been tested if Nup60 SUMOylation depends on Mms21.

Nuclear basket FG repeats are not required for Ty1 insertion

S. cerevisiae NPCs have eleven Nups, including three nuclear basket Nups (Nup1, Nup2 and Nup60), that contain unstructured FG repeat domains required for nucleocytoplasmic transport and maintaining the selective permeability barrier of NPCs (82–86). FG repeat motifs are defined as: FG, FxFG, GLFG; where x denotes any amino acid (87,88). Nup2 and Nup1 contain 16 and 23 FxFG peptide repeats, respectively, which serve as karyopherin docking sites (89–94). Nup60 contains four FxF repeats at its C-terminus (85). We acquired *nup1*, *nup2* and *nup60* strains carrying combinations of deletions in the FG repeats from Dr. Wente's lab (85). The Wente lab strain background is W303 which we found has undetectable levels of Ty1 transposition using the same conditions that enable transposition in the S288C background (growth at 20°C for 3 days). To increase Ty1 transposition levels in W303, we transformed the nuclear basket FG mutant yeast strains with a *pGAL-TyH3mHIS3AI-URA3* plasmid (pJBe376) and induced Ty1 element expression for 24 hours with 2% Gal media. We found that removal of the *nup1*, *nup2*, *nup60* nuclear basket FG repeats had no effect on the Ty1 targeting pattern and also did not significantly affect Ty1 insertion efficiency (Figure 12). A triple *nup1ΔFxFG nup2ΔFxFG nup60ΔFxF* strain deleted for all nuclear basket FG repeats demonstrated Ty1 insertion upstream of *tGLY* genes at 89% of wild type levels (Figure 12D). Our data implies that Nup1, Nup2 and Nup60 FG repeat domains, and therefore karyopherin docking at the nuclear basket, do not play a role in Ty1 targeting.

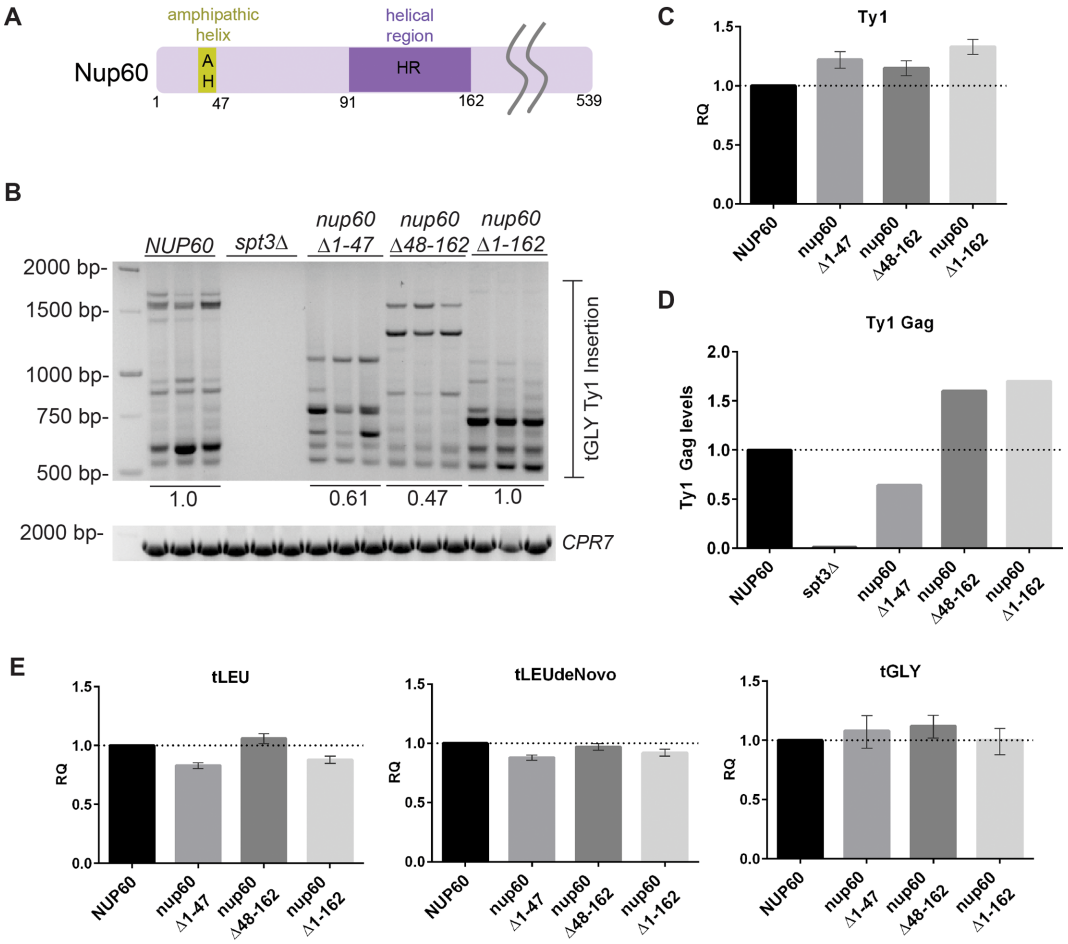

Figure 10. The Nup60 N-terminal AH and HR domains determine the pattern of Ty1 insertion upstream of *tGLY* genes. (**A**) Nup60 schematic with the AH and HR regions highlighted as in (46). (**B**) PCR amplification of endogenous Ty1 insertion levels in a *nup60Δ* yeast strain carrying a plasmid expressing either full-length nup60 (*NUP60*), nup60Δ1–47, nup60Δ48–162 or nup60Δ1–162 fused to mCherry. Genomic DNA was extracted from yeast strains grown for 3 days at 20°C. Amplification of a 2000 bp product containing the *CPR7* locus (lower panel) was performed as a control. Ty1 insertion levels, based on total number of bands and band intensities, were quantified using Image lab software. (**C**, **E**) Ty1 mRNA and tRNA (*tLEU*, *tLEU denovo*, *tGLY*) levels were normalized to a *TAF10* internal control and relative quantification (RQ) values were calculated based on wild type Ty1 mRNA or tRNA levels which were set to 1. qPCR was performed in triplicate. (**D**) Ty1 Gag (p49 and p45) protein levels measured with quantitative western blots relative to GAPDH used as a loading control, compared to wild type Gag/GAPDH levels, and presented in a bar graph.

The Ran binding domain of the mobile nucleoporin, Nup2, is essential for Ty1 insertion

Nup2 is a mobile Nup that is primarily located on the nuclear basket through a physical interaction with Nup60, but is also present in the nucleoplasm (47,91,95,96). We have shown that Ty1 insertion upstream of tRNA genes is reduced by ∼5-fold in the *nup2Δ* mutant whereas removal of the Nup2 FG repeats (*nup2ΔFxFG*) did not impact Ty1 insertion (Figures 6C, 7C and 12A). The C-terminus of Nup2 (aa583–720) contains a domain that binds the Ran small GTPase, called the Ran binding domain (RBD) (Figure 13A) (97). Ran, which is mostly GTP-bound in the nucleus, mediates release of nuclear protein cargo that transits through the NPC. The RBD also contributes to the interaction of Nup2 with the NPC as cells lacking the Nup2 RBD have a marked increase of Nup2 in the nucleoplasm (47). We found that a *nup2ΔRBD* yeast strain, engineered to lack residues 606–720 on Nup2, had a 50-fold reduction in Ty1 insertion compared to wild type (Figure 13B). Deletion of the Nup2 RBD did not cause a reduction in Ty1 mRNA expression or Ty1 Gag levels (Figures 13C and 13D). Although *tLEU* and *tLEU denovo* levels were similar to wild type, *tGLY* tRNA levels were reduced to 56% of wild type which is consistent with the role for Nup2 in docking tRNA genes at the NPC (Figure 13E) (21). The reduction in *tGLY* expression could explain a partial (50%) defect in Ty1 insertion, however the reduction of Ty1 insertion to almost background levels in the *nup2ΔRBD* strain suggests that mislocalization of Nup2 into the nucleoplasm, defects in Nup2 mediated nucleocytoplasmic transport, or disruption of the Ran-GTP gradient impairs Ty1 targeting.

The *S. cerevisiae* THO/TREX and TREX-2 NPC associated complexes can alter Ty1 insertion

We have demonstrated that the NPC nuclear basket impacts Ty1 element targeting upstream of tRNA genes. The nuclear basket has a variety of cellular roles including recruitment of actively transcribed genes to the NPC and coupling gene

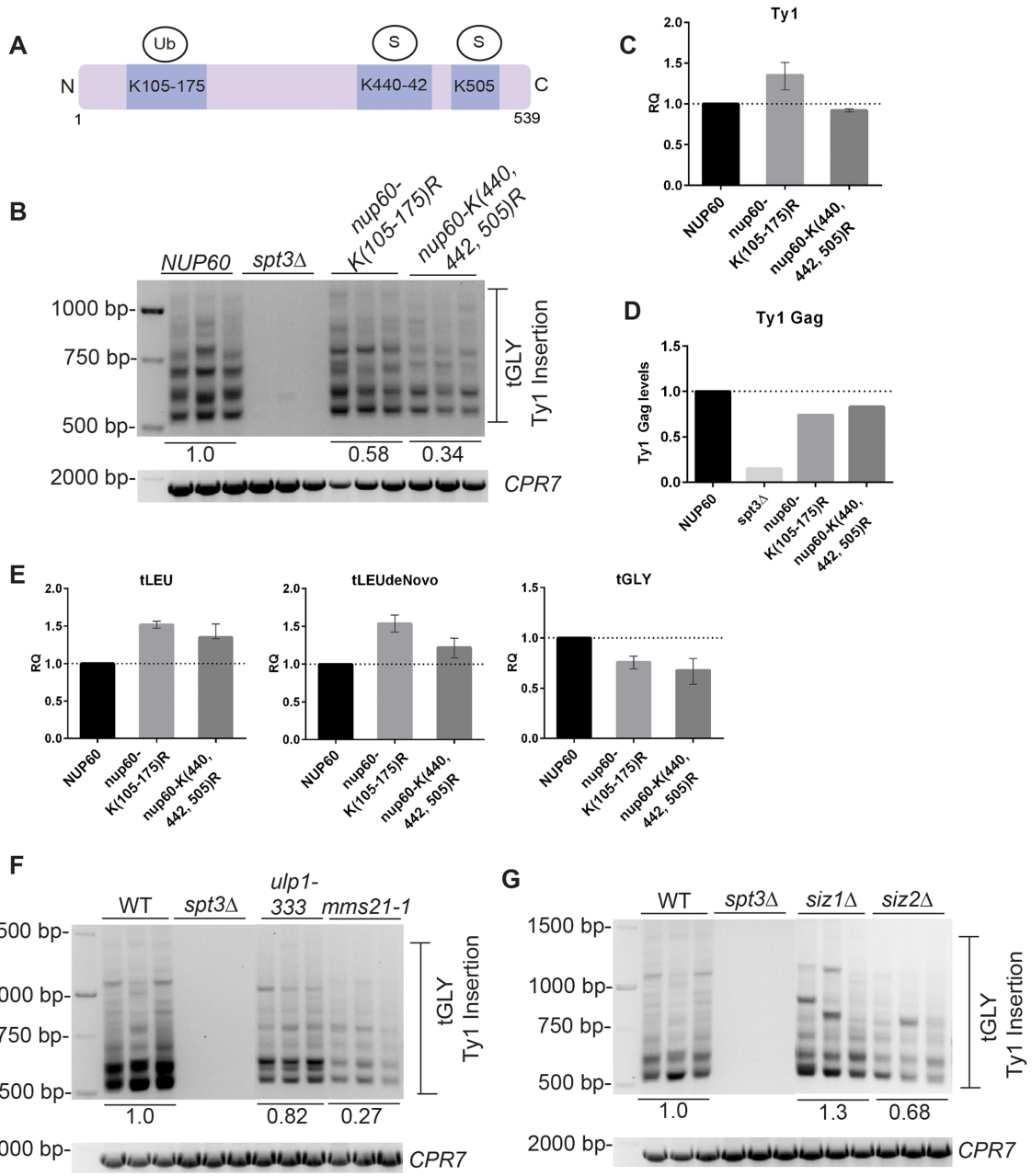

Figure 11. Nup60 SUMOylation and the SUMOylation pathway have a role in Ty1 insertion. (**A**) Schematic of Nup60 protein with Ub (K105–107) and SUMO (K440–442, K505) sites labeled as in (80). (**B**) PCR amplification of Ty1 insertion events upstream *tGLY* genes (GCC, 16 copies) in yeast strains carrying mutated Nup60 Ub (nup60-K(105–175)R) or SUMO (nup60-K(440, 442, 505)R sites assayed in triplicate. *spt3Δ* serves as a negative control. Image lab software was used to quantify total Ty1 insertion for each strain relative to wild type. A control *CPR7* is shown to confirm the presence of genomic DNA. (**C**) Ty1 mRNA in the indicated strains was assessed by qPCR relative to a *TAF10* control. The bar graph shows relative quantification (RQ) values of Nup60 mutants compared to wild type Ty1 mRNA which was set to 1. (**D**) Ty1 Gag (unprocessed or p49 and processed or p45) protein levels detected by western blot and quantified relative to GAPDH loading control in duplicate. The bar graph shows quantification of Ty1 Gag in mutant strains relative to wild type Ty1 Gag and GAPDH levels which was set to 1. (**E**) qPCR of *tLEU*, *tLEU denovo* and *tGLY*, relative to a *TAF10* control. RQ values are relative to wild type *tLEU*, *tLEU denovo*, or *tGLY* which were set to 1. (**F**) PCR amplification of Ty1 insertion upstream of *tGLY* in wild type (WT), *spt3Δ*, *ulp1–333* and *mms21–1* yeast strains. (**G**) PCR amplification of Ty1 insertion upstream of *tGLY* in WT, *spt3Δ*, *siz1Δ* and *siz2Δ* yeast strains. Ty1 insertion PCR gels in (F) and (G) were analysed as in (B).

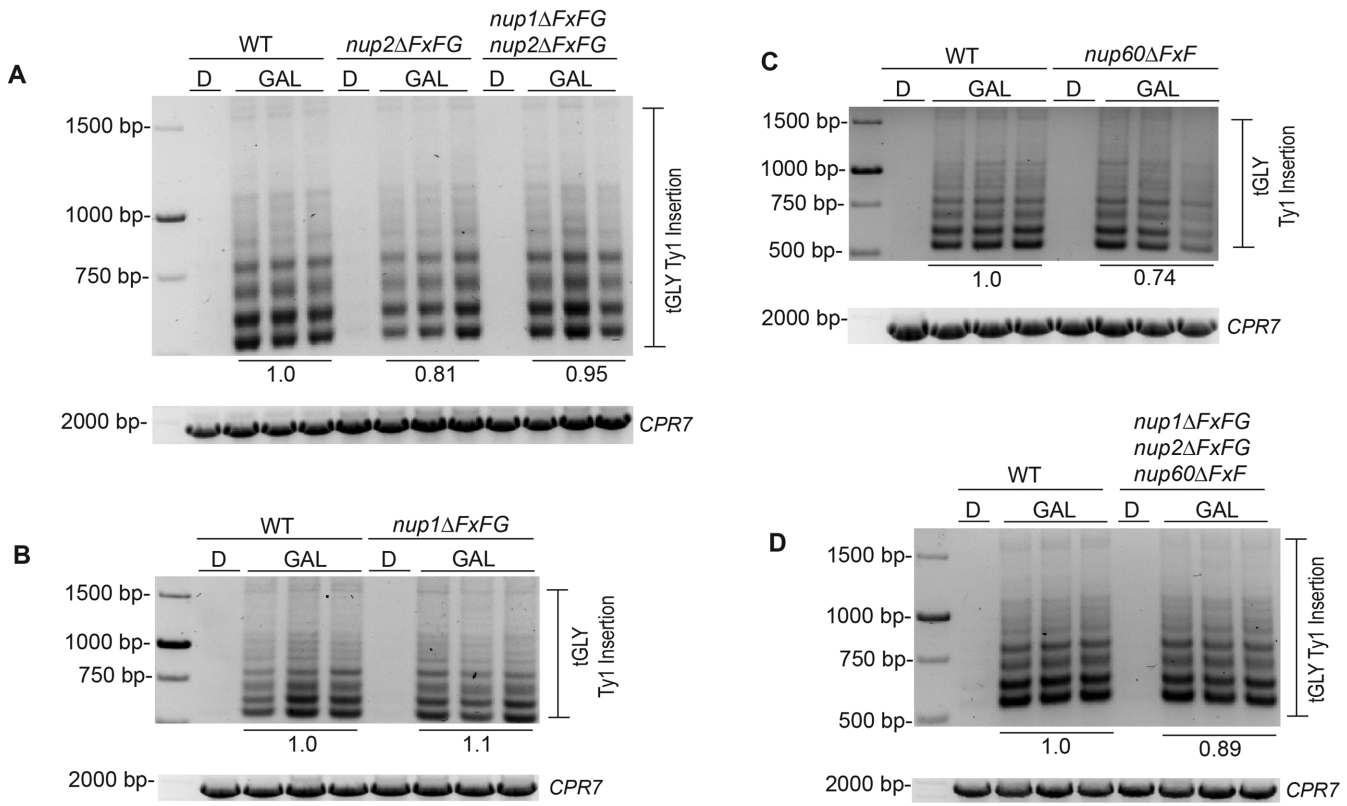

Figure 12. The nuclear basket FG repeats are not required for Ty1 insertion (**A–D**) *nup1ΔFxFG, nup2ΔFxFG*, *nup60ΔFxF*, *nup1ΔFxFG nup2ΔFxFG* and *nup1ΔFxFG nup2ΔFxFG nup60ΔFxF* yeast strains transformed with a *GAL-TY1* plasmid and grown in triplicate in galactose media (GAL) to induce Ty1 expression or dextrose media (D) as a negative control for 24 h at 25°C. Ty1 insertion was amplified at 16 *tGLY* (GCC) loci by PCR and Ty1 insertion levels were quantified by the number and intensity of insertions for each strain as compared to wild type (WT) which was set to 1. *CPR7* control PCR is shown in the lower panel for each gel.

transcription to nuclear mRNA export. Therefore, we explored the possibility that complexes that interact with the nuclear basket may have a role in Ty1 element targeting.

The evolutionary conserved THO/TREX (transcription-export) complex is composed of five tightly bound proteins that form the THO subcomplex (Hpr1, Mft1, Tho2, Thp2, Tex1) and interact with the Sub2 and Yra1 export factors to form TREX (Supplementary Figure S6A) (98–101). THO/TREX accompanies elongating RNA Polymerase II to couple mRNA biogenesis with nuclear export and recruits the mRNA export receptor Mex67-Mtr2 to the mRNA (Supplementary Figure S6A) (99,100,102). Mex67-Mtr2 binds to the mRNA to form a mRNP and also binds to the NPC to export the mRNP to the cytoplasm (103). We tested a subset of mutants in the THO/TREX complex for a Ty1 targeting phenotype. The *tho2Δ* and *mft1Δ* mutants had a ∼9-fold and 2-fold decrease respectively in Ty1 insertion upstream of *SUF16* compared to wild type (Supplementary Figure S6B). Conversely, the *hpr1Δ* mutant had a ∼2.8-fold increase in Ty1 insertion upstream of *SUF16* compared to wild type (Supplementary Figure S6B). Hpr1 is less stable than the other proteins in the THO/TREX complex and is targeted for degradation which is thought to control THO/TREX formation and mRNA export (104). Since degradation of Hpr1 is thought to promote dissociation of the THO/TREX complex it is not clear why *tho2Δ* and *mft1Δ* mutants have the opposite Ty1 insertion phenotype to *hpr1Δ* mutants. This said, deletion of Hpr1 also causes high frequencies of recombination and chromosome loss suggesting that Hpr1 plays a role in genome stability which could affect Ty1 replication (105,106).

The TREX-2 complex also functions to couple transcription with nuclear mRNA export (Supplementary Figure S6A) (98,107,108). In *S. cerevisiae* TREX-2 is composed of Cdc31, Thp1 and two copies of Sus1 linked to the core Sac3 protein (74,109). TREX-2 is involved in genome stability, DNA replication, transcription coupled mRNA export which includes the relocation of actively-expressed genes such as *GAL1* to the NE and binding to the NPC (20,107,109–113). Specifically, Sac3 binds the mRNA exporter Mex67-Mtr2 and requires Nup1 to tether to the NPC (Supplementary Figure S6A) (74). Sus1 is also a member of the SAGA complex; a large complex involved in chromatin remodeling and transcription activation (110). Sac3 binds to Sus1 and Cdc31 via the CID motif (Sac3 residues 733–860) and deletion of the Sac3 CID domain results in loss of Sus1 and Cdc31 from TREX-2, coupled with a defect in poly(A)+ RNA export and mislocalization of TREX-2 from NPCs (109,114). We acquired TREX-2 mutants from the Foiani lab which are in the W303 strain background and found, similar to the Wente lab strains, that the W303 wild type strain had very low levels of Ty1 insertion when com-

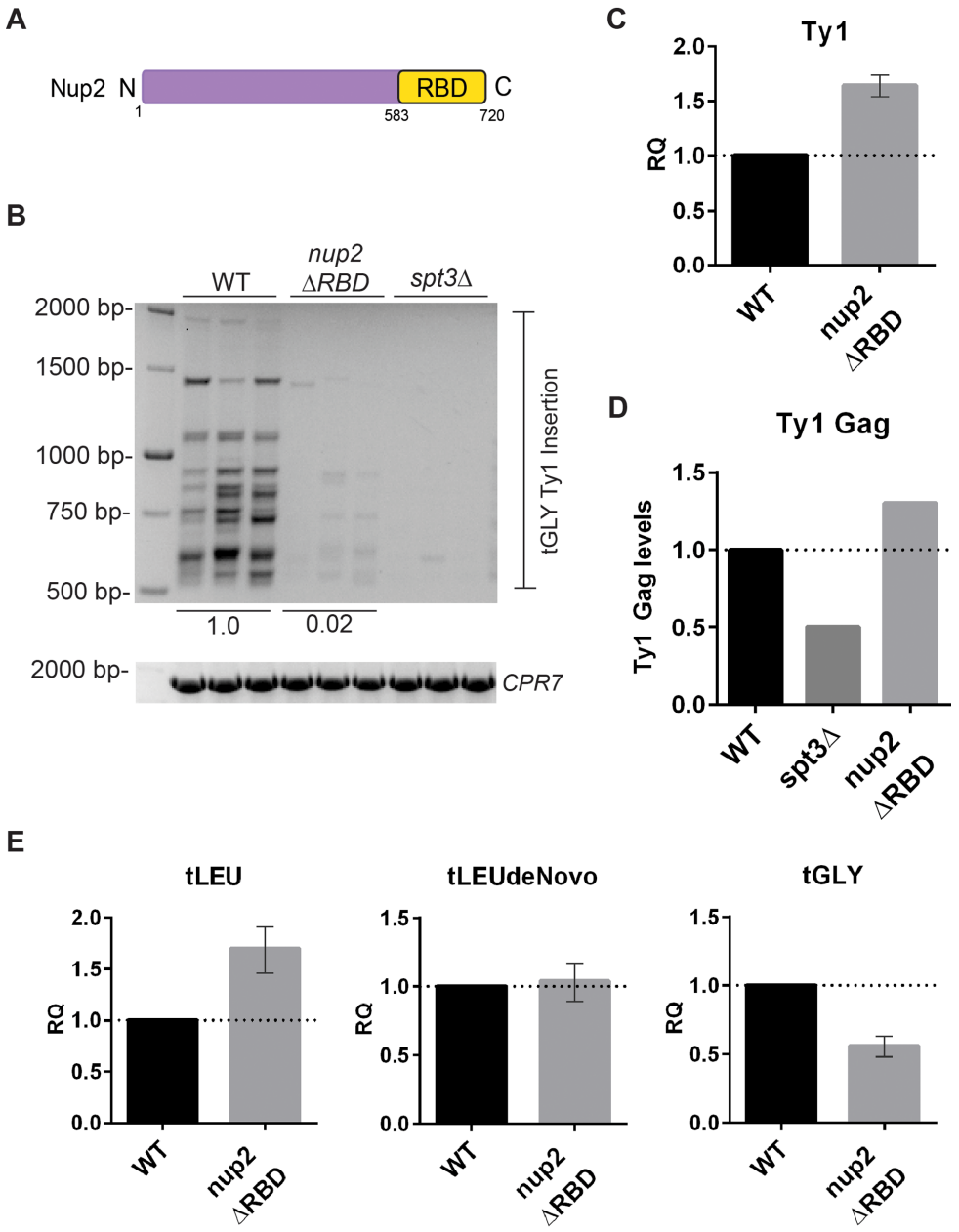

Figure 13. Removing the RBD of Nup2 abrogates Ty1 insertion. (**A**) Schematic of the Nup2 protein with the RBD shown in yellow (residues 583 to 720). (**B**) PCR amplification of Ty1 insertion upstream of 16 *tGLY* (GCC) genes in wild type (WT) and the nup2ΔRBD strains. *spt3Δ* is a negative control for Ty1 replication. Image lab software was used to quantify Ty1 insertion levels (number and intensity of bands) for each strain relative to WT which was set to 1. PCR amplification of the *CPR7* locus is shown for each sample to verify the isolation of PCR quality genomic DNA. (**C**, **E**) Relative quantification (RQ) of Ty1 mRNA levels and *tLEU*, *tLEU denovo*, *tGLY*, respectively, relative to a *TAF10* control as measured by qPCR in triplicate. RQ values are relative to WT Ty1 mRNA or wild type *tLEU*, *tLEU denovo* or *tGLY* which were set to 1. (**D**) Bar graph of Ty1 Gag (unprocessed or p49 and processed or p45) protein levels quantified relative to a GAPDH loading control in duplicate by western blot. Whole cell extracts were processed from yeast strains grown to log phase. Quantification values are relative to WT Ty1 Gag and GAPDH levels which was set to 1.

pared to the S288C wild type strain (Supplementary Figure S6C). However, we were able to detect Ty1 transposition in the TREX-2 mutants because the *sac3Δ* mutant and the *sac3ΔCID* mutant had a 14-fold and ∼24-fold increase in Ty1 insertion upstream of *tGLY* genes, respectively (Supplementary Figure S6C). As well, the *sus1Δ* mutant had a ∼19-fold increase in Ty1 insertion upstream of *tGLY* genes (Supplementary Figure S6C). Another interesting feature of the TREX-2 mutants was that the pattern of Ty1 insertion differed between the *sac3Δ*, *sac3ΔCID* and *sus1Δ* mutant although we were not able to compare to a wild type strain. Our data suggests that the presence of TREX-2 may interfere with Ty1 insertion and that removal of TREX-2 from the NPC may impact chromatin arrangement, similar to what we detected with the Nup1 and Nup60 AH and HR mutants. Another possibility is that the increased Ty1 inser-

tion in the TREX-2 mutants is due to cellular stress caused by genome instability or defects in DNA replication or transcription. Taken together, our analysis of THO/TREX and TREX-2 suggest that neither of these NPC associated complexes are required for Ty1 transposition and their presence may impede the insertion of Ty1 elements into the genome.

Ty1 insertion is retargeted to sub-telomeric regions in nuclear basket mutants

The *nup1Δ* and *nup2Δ* mutants have wild type Ty1 mobility yet reduced Ty1 targeting upstream of *tGLY* genes suggesting that Ty1 insertion is occurring elsewhere in the genome. It has previously been shown that Ty1 elements are redirected to telomere-proximal regions when the *S. cerevisiae* Rpc40 protein is substituted for the *S. pombe* Rpc40 protein which no longer interacts with Ty1-IN (7). We tested if Ty1 elements are mis-targeted to telomere-proximal regions in nuclear basket deletion mutants with primers that hybridize to Ty1 insertion sites identified in the *Bridier-Nahmias et al*. study that are near chromosome ends (7). The insertion sites are located in genes with nearly identical homologues (*SNZ2*/*SNZ3* and *HXT15*/*HXT16*) therefore each set of PCR reactions amplifies Ty1 elements at two sub-telomeric regions (8). As a control, we induced endogenous Ty1 transposition in the *S. cerevisiae RPC40* and *S. pombe RPC40* strains which have previously been shown to accumulate Ty1 elements at telomere-proximal regions only in the *S. pombe RPC40* strain (Figure 14) (7,8). When compared to the *S. cerevisiae RPC40* strain the yeast strain carrying the *S. pombe RPC40* had ∼33–69 times higher Ty1 insertion at the *SNZ2*/*SNZ3* loci (Chr XIV left end/Chr VI left end) and ∼18–51 times higher Ty1 insertion at *HXT15*/*16* loci (Chr IV left end and Chr X right end) (Figure 14). We found that Ty1 elements are indeed mis-targeted to the chromosome ends in *nup1Δ*, *nup2Δ*, *mlp1Δ* and *mlp2Δ* mutants but not in a wild type strain (Figures 14A and 14B). When compared to wild type or *spt3Δ* strains which both have minimal insertion at sub-telomere regions, *mlp1Δ* strains had a ∼33-fold and *mlp2Δ* strains had a ∼25-fold increase in Ty1 insertion at *SNZ2*/*SNZ3* loci and an even higher increase in Ty1 insertion at *HXT15*/*HXT16* loci (Figure 14). Removal of Nup1 caused a more modest increase in Ty1 insertion (∼6–8 times) whereas the *nup2Δ* strain had a ∼22 to 39-fold increase in Ty1 insertion at the sub-telomere regions (Figure 14). Even though *nup60Δ* mutants express Ty1 elements at low levels (Figure 2A), we also detected mis-targeting to the *SNZ2*/*SNZ3* gene and a few insertion events at the *HXT15*/*HXT16* locus (Figure 14A). In summary, our data suggests that the nuclear basket is required for targeting of Ty1 elements upstream of tRNA genes and for preventing insertion at chromosome ends.

DISCUSSION

In the mid 1980s, Blobel postulated the 'gene gating' hypothesis, asserting that actively transcribed genes are tethered at NPCs to allow transcription and mRNA export to be coupled events (115). This hypothesis sparked exploration of transport-independent functions of NPCs resulting in mounting evidence supporting the influence of NPCs on chromatin structure and organization which in turn can affect gene regulation in yeast and higher order eukaryotes (13). Active transcription of at least a subset of genes has been demonstrated to occur at NPCs in a variety of eukaryotic organisms (25,74,107,116–123). Of particular importance to this study is that tRNA genes, the preferred genomic target of Ty1, are actively transcribed at NPCs during the peak of tRNA synthesis (M phase of the cell cycle) (21). Moreover, three studies have reported that mutations of a sub-set of Nups cause nuclear retention of intron-containing tRNAs (75,124,125). Given this functional link between Nups, chromatin, and transcription, we explored the role of Nups in Ty1 element integration into the genome.

In this study, we surveyed a panel of 19 NPC mutants for quantitative defects in Ty1 mobility and identified 11 mutants with a statistically significant difference in Ty1 mobility (Figure 1). The majority of these Nups were subunits of the Nup170 inner ring complex and the nuclear basket, however Nup mutants from all NPC substructures impacted Ty1 transposition (Figure 1, Table 1). Most Nup mutants with reduced Ty1 mobility also displayed decreased insertion of Ty1 elements upstream of the *SUF16* and *SUP61* tRNA genes (Figures 1, 4, 5, Table 1). We were surprised to discover, however, that Nup mutants with wild type levels of Ty1 mobility also had defects in Ty1 targeting upstream of the *SUF16* and *SUP61* genes (Figures 1, 6, 7 and Table 1). Included in this group are two nuclear basket mutants, *nup1Δ* and *nup2Δ* and due to the proximity of the nuclear basket Nups to chromatin we focused our study on this complex. We have demonstrated that deletion of individual nuclear basket genes affects Ty1 mRNA expression (*nup60Δ*), Ty1 mobility (*nup60Δ*, *mlp1Δ*, *mlp2Δ*) and Ty1 targeting (*nup1Δ*, *nup2Δ*, *nup60Δ*, *mlp1Δ*, *mlp2Δ*) (Figures 1, 2A, 4–8, 14). The FG repeat domains of Nup1, Nup2 and Nup60 are not required for Ty1 targeting, instead the AH and HR N-terminal domains of Nup1 and Nup60 as well as the C-terminal RBD of Nup2 are important for accurate Ty1 insertion (Figures 9, 10, 12 and 13). Finally, in the absence of nuclear basket proteins, Ty1 elements are mis-targeted to telomere-proximal regions (Figure 14).

We discovered that the Nup60 nucleoporin has a role in Ty1 mRNA expression that resulted in reduced Ty1 Gag levels (Figure 2A and B). Chromatin immunoprecipitation experiments have demonstrated that Nup60 can interact with chromatin (58,126) and specifically tRNA genes (21). There are at least nine transcription factors that bind to the Ty1 promoter and three chromatin-remodeling complexes including SAGA (5). SAGA and TREX-2 share a common subunit, Sus1, which is part of the deubiquitylation module (DUB) of the SAGA complex that also contains Ubp8, Sgf11 and Sgf73 (107). We found that, in the W303 strain background, a *sus1Δ* mutant had ∼19-fold increased Ty1 insertion upstream of *tGLY* genes when compared to the wild type strain (Supplementary Figure S6C). Although SAGA subunits such as Spt3 are clearly required for Ty1 transcription our data suggests that the DUB module is not. We also demonstrated that mutation of the TREX-2 protein Sac3 results in an increase of Ty1 insertion upstream of *tGLY* genes (Supplementary Figure S6C). Of the nine transcription factors that modulate Ty1 transcription, the Rap1 and Gcr1 transcriptional coactivators interact with

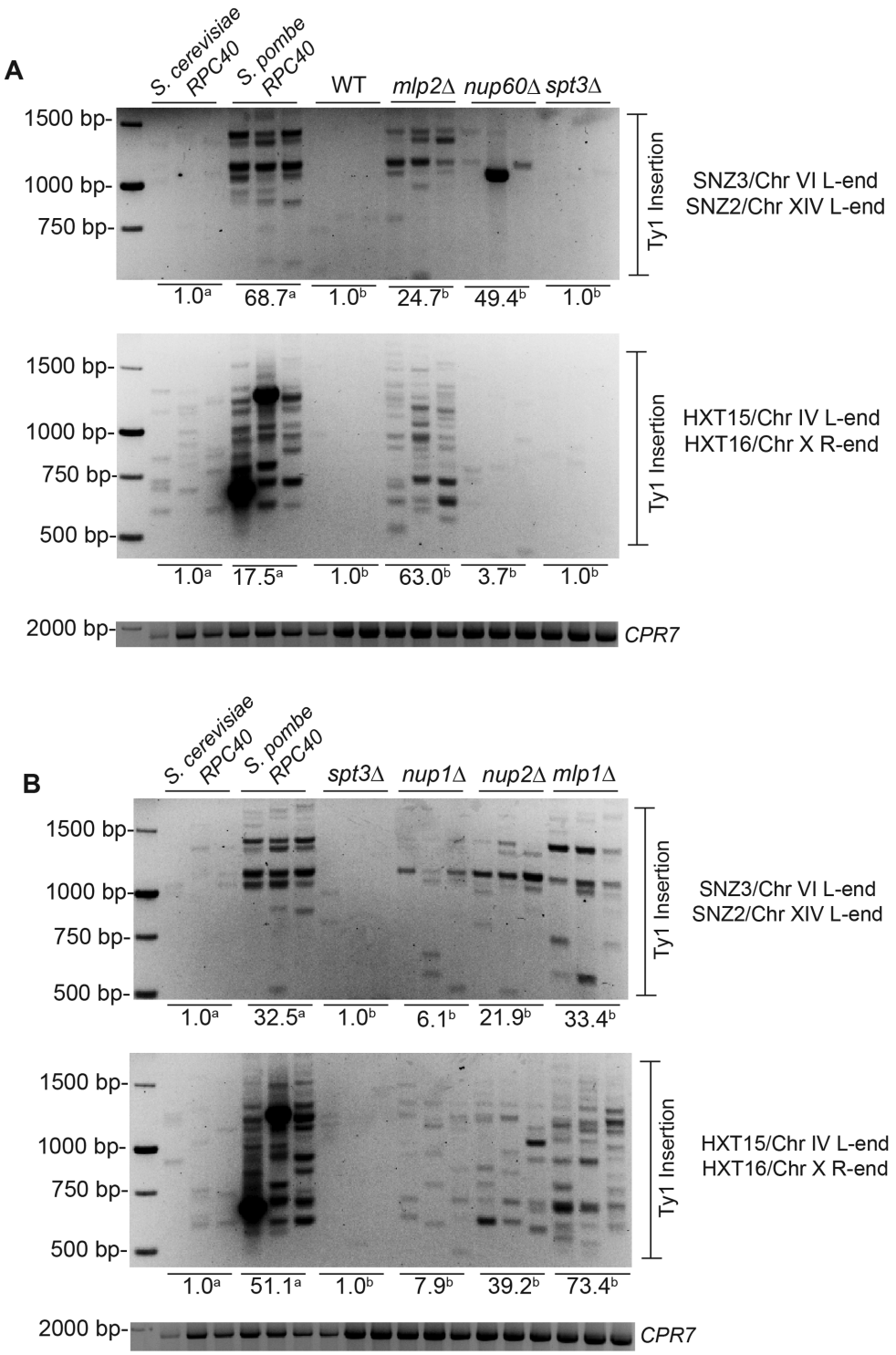

Figure 14. Ty1 is targeted to sub-telomeres in the absence of nuclear basket proteins**.** PCR amplification of Ty1 insertion events from genomic DNA extracted from (**A**) control strains [*S. cerevisiae RPC40*, *S. pombe RPC40*, wild type (WT), *spt3Δ*] and nuclear basket deletion strains (*mlp2Δ*, *nup60Δ*) or (**B**) control strains (*S. cerevisiae RPC40*, *S. pombe RPC40*, *spt3Δ*) and nuclear basket deletion strains (*nup1Δ*, *nup2Δ*, *mlp1Δ*) grown for 3 days at 20°C. Each PCR contained a Ty1 element primer and a sub-telomere-proximal primer; the sub-telomere-proximal primers hybridize to two identical genomic regions at *SNZ3*/*SNZ2* or *HXT15*/*HXT16* loci. *CPR7* control PCR is shown to demonstrate the presence of genomic DNA in each sample. Ty1 insertion levels were quantified based on the number of bands and band intensity for the *S. pombe RPC40* positive control relative to the *S. cerevisiae RPC40* which was set to 1.0 (denoted as 1.0^{a}). Each Nup basket deletion strain was compared to WT or *spt3Δ*, which were set to 1.0 (denoted as 1.0^{b}). Chr, chromosome, R, right; L, left.

the Nup84 complex (123). Rap1 also interacts with Nup170 (26). However, a Nup84 complex mutant (*sec13-1*) and the *nup170Δ* mutant both had wild type levels of Ty1 mRNA suggesting that these Nup interactions are not required for Ty1 expression (Figure 2A). Therefore, it remains to be determined which Ty1 transcription factor may interact with Nup60 or if Nup60 itself has a role in transcriptional activation.

We observed defects in Ty1 mobility in a subset of mutants from every NPC complex, except for the one central FG Nup we tested (*nup100Δ*) (Figure 1, Table 1). Every mutant we tested in the Nup170 inner ring complex, except for *nup59Δ*, had greatly reduced Ty1 mobility and negligible insertion of Ty1 elements upstream of the *SUF16* or *SUP61* tRNA genes (Figures 1, 4, 5, Table 1). Nup170 interacts with genomic regions containing ribosomal protein and subtelomeric genes to mediate nucleosome positioning and transcription repression (26). Ty1 insertion in an RNA pol III mutant has been shown to be redirected to subtelomeric loci (7) which could involve Nup170, given its role in chromatin organization of this region. We also demonstrated that in the absence of nuclear basket proteins, Ty1 insertion is re-targeted to subtelomeric regions (Figure 14). It will be interesting to determine if Ty1 re-targeting in the nuclear basket mutants depends on the presence of Nup170.

Mutation of the Nup84 outer ring complex resulted in variable Ty1 mobility defects with an 8-fold reduction in the *sec13-1* mutant, a 3.5-fold increase in the *nup120Δ* mutant and wild type Ty1 mobility in the *nup84Δ* and *nup133Δ* strains (Figure 1B, Table 1). All Nup84 outer ring mutants, however, displayed defects in Ty1 targeting upstream of the *SUF16* and *SUP61* genes (Figures 4A-B, 5A-B, 6A and 7A). As predicted from the increase in Ty1 cDNA and Ty1 mobility, the *nup120Δ* mutant had a ∼10-fold increase in Ty1 targeting mostly in the second nucleosome upstream of the *SUF16* gene (asterisk, Figure 4B). We also detected ∼2.4-fold increased Ty1 insertion upstream of the *SUP61* gene in the *nup120Δ* mutant but no specific nucleosome position was targeted (Figure 5B). This may reflect a difference in NPC interactions with the pericentromere (where *SUF16* is located on Chr. III) versus the chromosome arm (where *SUP61* is located on Chr. III). Another interesting observation was that in the *nup84Δ* mutant, Ty1 elements were targeted into a non-canonical position in the second nucleosome (arrow, Figure 6A) and in the *nup133Δ* mutant Ty1 elements were primarily targeted to the first nucleosome (asterisk, Figure 6A). It is important to mention that deletion mutations of *NUP84*, *NUP133* or *NUP120* cause NPC clustering (33,34,127–129) while the *NUP188* deletion mutant has defects in NE morphology (130). Global structural changes in NPCs could in turn affect chromatin organization and the positioning of actively transcribed genes which may explain the alterations of Ty1 insertion in these Nup mutant strains.

We focused our study on the NPC nuclear basket proteins, which are reported in numerous studies to interact with chromatin (24,77,78). Ty1 insertion into the genome was nearly abolished in the *nup60Δ* mutant, likely due to the low levels of Ty1 mRNA and Gag expression (Figures 2, 4C and 5C). We acquired mutants in two Nup60 N-terminal helical domains from the Kohler lab in an attempt to identify a *NUP60* mutant that did not interfere with Ty1 mRNA expression. The Kohler lab previously demonstrated that removal of the Nup60 AH (nup60Δ1–47) or Nup60 HR (nup60Δ48–162) led to a partial detachment of Nup60 from the nuclear basket, and the deletion of both HRs (nup60Δ1–162) caused nearly complete mislocalization of Nup60 (46). Unlike the *nup60Δ* yeast strain, the Nup60 AH and HR mutants generated wild type levels of Ty1 mRNA, Ty1 Gag and tRNA genes which allowed us to test for Ty1 element targeting in the Nup60 AH and HR mutants (Figure 10). The fact that the nup60Δ1–162 mutant, which almost completely detaches from the NPC, expresses Ty1 mRNA at wild type levels, also raised the question of whether or not recruitment to the NPC is necessary for Ty1 mRNA expression (46). We find that Ty1 elements are able to insert upstream of *tGLY* genes in all three Nup60 AH and HR mutants, however the pattern of Ty1 targeting is altered (Figure 10B). Docking of tRNAs at the NPC requires Nup60 (21) and we find that *nup60Δ* mutants have a 50% reduction in *tLEU* and *tGLY* gene expression (Figure 3). Hence, there may be changes in the chromatin and nucleosome positioning upstream of tRNAs in the Nup60 AH and HR mutants that causes changes in Ty1 targeting, although expression of *tLEU*, *tLEU denovo* and *tGLY* are not affected in these mutants.

Similar to Nup60, Nup1 also has an AH and HR domain in its N-terminus that interacts with the inner nuclear membrane to promote curvature (46). We found that the Nup1 AH (nup1Δ1–32) and HR (nup1Δ85–123) mutants had Ty1 mRNA, Ty1 Gag and tRNA levels similar to wild type but a change in the Ty1 insertion pattern upstream of *tGLY* (Figure 9). The nup1Δ1–32 mutant that lacks the AH, had ∼11-fold increased Ty1 insertion at the second nucleosome position upstream of *tGLY* genes whereas the nup1Δ85–123 mutant that lacks the HR had ∼1.8-fold increased Ty1 insertion targeted approximately five nucleosomes upstream of the tRNA gene (Figure 9B). Both the AH and HR regions contribute to Nup1 NPC localization as removing the AH (nup1Δ1–32) causes a slight mislocalization of Nup1 into the nucleoplasm which is increased when removing the HR (nup1Δ85–123) (46). The Ty1 targeting patterns in Nup1 and Nup60 AH/HR mutants point to a role for NPC proximal membrane curvature in the accurate targeting of Ty elements likely due to the role of Nup60, and probably Nup1, in recruitment of tRNA genes to the NPC.

Monoubiquitylation of Nup60 plays a role in tethering both Nup60 and Nup2 to the NPC (80). Nup60 is also SUMOylated however the function of the Nup60 SUMO modification is not yet known (80). We found that Ty1 insertion in the Nup60 ubiquitin-deficient mutant [nup60-K(105–175)R] is reduced to 58% of wild type level which may be because this mutant displays increased dissociation from the NPC (80). Interestingly, Ty1 insertion was reduced to 34% of wild type levels in the Nup60 SUMOylation mutant [nup60-K(440,442,505)R] (Figure 11B). Detection of Nup60 SUMOylation requires mutation of the Ulp1 protease and the SUMO ligases Siz1 and Siz2 are required for Nup60 SUMOylation in the *ulp1* background (80). We tested deletions of the three mitotic E3 SUMO ligases (Siz1, Siz2, Mms21) and found that the *mms21–1* mutant had the greatest reduction in Ty1 insertion (Fig-

ure 11F). Mms21 is a component of the Smc5/6 complex that functions in DNA repair and genome integrity, particularly at the ribosomal DNA locus (131,132). SUMOylation of RNA Pol III subunits is important for Pol III assembly and recruitment to tRNA genes but the E3 ligase responsible for Pol III SUMOylation has not yet been identified (133,134).Therefore SUMOylation is likely to affect multiple proteins involved in Ty1 targeting to the genome, including Nup60 and possibly other NPC and RNA Pol III proteins.

We next explored if other regions of the nuclear basket proteins are involved in Ty1 targeting. Nup1, Nup2 and Nup60 all contain FG repeats that bind cargo for facilitated transport across the NPC (85,88). We did not detect a defect in Ty1 insertion upstream of *tGLY* genes in any single FG repeat mutant or even the triple *nup1ΔFxFG nup2ΔFxFG nup60ΔFxFG* mutant (Figure 12). Therefore, the FG repeat cargo binding capacity of the nuclear basket is not required for Ty1 element targeting into the genome. Ty3 transposition is also not affected in *nup1ΔFxFG*, *nup2ΔFxFG* and *nup60ΔFxFG* single mutants (35). Instead, Ty3 Gag interacts with Nup GLFG repeats to allow docking of the Ty3 VLP onto the NPC (35). Whether or not Ty1 VLPs also dock onto the NPC remains to be determined.

Unlike the nuclear basket proteins, Nup2 is transiently associated with NPCs, sharing the roles of NPC component and soluble transporter (84,89,92,95). Upon binding near the promoter regions of genes, Nup2 transports active genes to NPCs (20,25,58,135). Nup2, along with the tRNA exporter Los1, also participates in recruitment of tRNA genes to the NPC (21). We find that when Nup2 is deleted, Ty1 mobility remains normal but Ty1 insertion upstream of tRNA genes is decreased (Figures 1B, 6C, 7C, Supplementary Figure S5A). Given that Ty1 mRNA levels are normal in the *nup2Δ* yeast strain, the decreased Ty1 insertion at tRNA genes could be partially due to the reduced transcription of tRNA genes (Supplementary Figure S5B and S5C). Nup2 contains a RBD and localization of Nup2 to the nuclear face of the NPC requires Ran-GTP binding (90). We find that removing the RBD of Nup2 reduced Ty1 element insertion upstream of *tGLY* genes by 50-fold but did not affect Ty1 mRNA or Gag levels and only reduced *tGLY* levels by ∼50% (Figure 13). Nup2 could be acting as a gene-NPC tether or mediator in this process given the potential role of Nup2 in nuclear export of tRNAs as Nup2 interacts with the tRNA exportin, Los1 (136). Removing or altering Nup2, and other nuclear basket Nups, could affect the cell cycle as the NPC-tRNA interaction occurs more frequently during M phase (21). Furthermore, perturbing the interaction of NPC-gene tethering could result in changes to chromatin organization or the loss of complexes localizing to the nuclear periphery both of which could have broad cellular effects on processes such as transcription and nucleocytoplasmic transport.

Although *nup1Δ* and nup2Δ cells had wild type Ty1 mobility as well as Ty1 mRNA and Gag levels, Ty1 insertion upstream of *tGLY* was reduced (Figures 1B, 6C, 7C and 8). It has previously been demonstrated that a strain expressing *S. pombe* Rpc40 that no longer interacts with Ty1-IN targets Ty1 elements to subtelomeric regions (7). We find that Ty1 elements are mis-targeted to the same subtelomeric regions in *nup1Δ* and *nup2Δ* mutants (Figure 14). We also detect Ty1 mis-targeting to subtelomeric regions in *mlp1Δ* and *nup60Δ* mutants that have low Ty1 mobility and the *mlp2Δ* mutant that has increased Ty1 mobility (Figures 1 and 14). Notably, the subtelomeric regions do not contain Pol III genes and our wild type strain does not target Ty1 elements to chromosome ends (Figure 14). We suspect that in the absence of nuclear basket proteins, another NPC protein is directing Ty1 elements into the genome such as Nup170 which interacts with subtelomeric chromatin (26). We have not yet tested if Ty1-IN interacts with Pol III subunits in our nuclear basket mutant strains. However, we think that an interaction between Ty1-IN and nuclear basket proteins is likely transient, because in our previous purification of Ty1-IN, followed by mass spectrometry analysis, we did not identify an enrichment of Nup proteins whereas we did identify Pol III subunits (8). We propose a model whereby tRNA genes are transcribed by Pol III at the NPC concurrent with the PIC complex moving through the same pore or a nearby pore. In this scenario, both the tRNA gene target and the PIC complex would be in close physical proximity to undergo Ty1-IN-dependant DNA joining reactions. Presumably, Nups could tether the PIC to chromatin. Whether Nups interact directly with Ty1-IN or act as a bridge between Ty1-IN and other factors such as subunits of the Pol III complex remains to be determined.

In summary, our results indicate that components of the nuclear basket such as Nup1, Nup2 and Nup60, couple tRNA expression, Ty1 expression and Ty1 integration. Future work will establish if the nuclear basket and the Ty1 machinery interact directly or indirectly by impacting on other cellular processes such as nucleocytoplasmic transport.

Functional conservation of Ty1-IN with HIV-1 IN suggests that studies of Ty1-IN protein interactions and targeting in yeast will be applicable to the mechanism of HIV-1 propagation. Indeed, three independent genome-wide siRNA screens for HIV-1 host factors identified Nups involved in PIC trafficking and integration, suggesting a model of 'import-coupled integration' (43–45). Follow-up work has shown that the HIV-1 capsid interacts with human Nups, such as Nup153, and when this interaction is inhibited HIV-1 infectivity is significantly reduced (137–139). Interestingly, HIV-1 integration has been shown to predominantly occur in chromatin located at the outer edge of the nucleus, in close proximity with nuclear pores (140,141). Moreover, two groups found that HIV-1 associates with the NE in the cytoplasm and preferentially integrates at chromatin close to the NE (142,143). These studies, along with our own, highlight a role for NPCs in dictating integration of yeast retrotransposons or mammalian retroviruses either through direct PIC interactions or as a result of indirect effects on chromatin organization.

SUPPLEMENTARY DATA

Supplementary Data are available at NAR Online.

ACKNOWLEDGEMENTS

We thank Dr Jef Boeke (Institute for Systems Genetics, New York University) for the anti-Gag sera and Ty1 plasmids

(pJBe376 and pJEF724). We thank Dr Chris Walkey (UBC Wine Research Centre) for the pCW1 vector. We also acknowledge the Centre for Drug Research and Development (CDRD) for the use of their Typhoon Imager. We thank Dr Thibault Mayor and Dr Sophie Comyn at the Michael Smith Laboratories (MSL) (UBC) for the use of their Bio-Rad Gel Doc and Odyssey CLx imaging system. We thank Dr Phil Hieter at the MSL (UBC) for yeast strains. We sincerely thank the following investigators for yeast strains and plasmids: Dr Anita H. Corbett (Emory University) for Nab2 mutants, Dr Alwin Köhler (Max F. Perutz Laboratories, Medical University of Vienna) for Nup60 and Nup1 helical mutant plasmids, Dr Marco Foiani (Fondazione Istituto FIRC di Oncologia Molecolare (IFOM) at IFOM-IEO Campus Milan) for TREX-2 mutant yeast strains, Dr Susan R. Wente (Vanderbilt) for the ΔFG yeast strains, Dr Catherine Dargemont (University Paris Diderot) for Nup60 ubiquitin and SUMO mutants, Dr Katja Sträßer (Justus Liebig University Giessen) NAB2 yeast strain and *nab2–34* plasmid, and Dr John D. Aitchison (Institute for Systems Biology, Seattle) for the *nup2ΔRBD* yeast strain. We also thank Anna Zheltukhina and Braydon Pacheco for preparing media.

FUNDING

Canadian Institutes of Health Research [HOP-131559 to V.M.]. Funding for open access charge: Canadian Institutes of Health Research [HOP-131559].
Conflict of interest statement. None declared.

REFERENCES

1. Lewis,P.F. and Emerman,M. (1994) Passage through mitosis is required for oncoretroviruses but not for the human immunodeficiency virus. *J. Virol.*, **68**, 510–516.
2. Roe,T., Reynolds,T.C., Yu,G. and Brown,P.O. (1993) Integration of murine leukemia virus DNA depends on mitosis. *EMBO J.*, **12**, 2099–2108.
3. Lewis,P., Hensel,M. and Emerman,M. (1992) Human immunodeficiency virus infection of cells arrested in the cell cycle. *EMBO J.*, **11**, 3053–3058.
4. Weinberg,J.B., Matthews,T.J., Cullen,B.R. and Malim,M.H. (1991) Productive human immunodeficiency virus type 1 (HIV-1) infection of nonproliferating human monocytes. *J. Exp. Med.*, **174**, 1477–1482.
5. Curcio,M.J., Lutz,S. and Lesage,P. (2015) The Ty1 LTR-Retrotransposon of Budding Yeast, Saccharomyces cerevisiae. *Microbiol. Spectr.*, **3**, doi:10.1128/microbiolspec.MDNA3-0053-2014.
6. Devine,S.E. and Boeke,J.D. (1996) Integration of the yeast retrotransposon Ty1 is targeted to regions upstream of genes transcribed by RNA polymerase III. *Genes Dev.*, **10**, 620–633.
7. Bridier-Nahmias,A., Tchalikian-Cosson,A., Baller,J.A., Menouni,R., Fayol,H., Flores,A., Saïb,A., Werner,M., Voytas,D.F. and Lesage,P. (2015) Retrotransposons. An RNA polymerase III subunit determines sites of retrotransposon integration. *Science*, **348**, 585–588.
8. Cheung,S., Ma,L., Chan,P.H., Hu,H.L., Mayor,T., Chen,H.T. and Measday,V. (2016) Ty1-Integrase interacts with RNA Polymerase III specific subcomplexes to promote insertion of Ty1 elements upstream of Pol III-transcribed genes. *J. Biol. Chem.*, **291**, 6396–6411.
9. McLane,L.M., Pulliam,K.F., Devine,S.E. and Corbett,A.H. (2008) The Ty1 integrase protein can exploit the classical nuclear protein import machinery for entry into the nucleus. *Nucleic. Acids. Res.*, **36**, 4317–4326.
10. Moore,S.P., Rinckel,L.A. and Garfinkel,D.J. (1998) A Ty1 integrase nuclear localization signal required for retrotransposition. *Mol. Cell. Biol.*, **18**, 1105–1114.
11. Kenna,M.A., Brachmann,C.B., Devine,S.E. and Boeke,J.D. (1998) Invading the yeast nucleus: a nuclear localization signal at the C terminus of Ty1 integrase is required for transposition in vivo. *Mol. Cell. Biol.*, **18**, 1115–1124.
12. Le Sage,V. and Mouland,A.J. (2013) Viral subversion of the nuclear pore complex. *Viruses*, **5**, 2019–2042.
13. Ibarra,A. and Hetzer,M.W. (2015) Nuclear pore proteins and the control of genome functions. *Genes Dev.*, **29**, 337–349.
14. Timney,B.L., Raveh,B., Mironska,R., Trivedi,J.M., Kim,S.J., Russel,D., Wente,S.R., Sali,A. and Rout,M.P. (2016) Simple rules for passive diffusion through the nuclear pore complex. *J. Cell Biol.*, **215**, 57–76.
15. Wente,S.R. and Rout,M.P. (2010) The nuclear pore complex and nuclear transport. *Cold Spring Harb. Perspect. Biol.*, **2**, a000562.
16. Grossman,E., Medalia,O. and Zwerger,M. (2012) Functional architecture of the nuclear pore complex. *Annu. Rev. Biophys.*, **41**, 557–584.
17. Fischer,J., Teimer,R., Amlacher,S., Kunze,R. and Hurt,E. (2015) Linker Nups connect the nuclear pore complex inner ring with the outer ring and transport channel. *Nat. Struct. Mol. Biol.*, **22**, 774–781.
18. Stuwe,T., Bley,C.J., Thierbach,K., Petrovic,S., Schilbach,S., Mayo,D.J., Perriches,T., Rundlet,E.J., Jeon,Y.E., Collins,L.N. *et al.* (2015) Architecture of the fungal nuclear pore inner ring complex. *Science*, **350**, 56–64.
19. Amlacher,S., Sarges,P., Flemming,D., van Noort,V., Kunze,R., Devos,D.P., Arumugam,M., Bork,P. and Hurt,E. (2011) Insight into structure and assembly of the nuclear pore complex by utilizing the genome of a eukaryotic thermophile. *Cell*, **146**, 277–289.
20. Casolari,J.M., Brown,C.R., Komili,S., West,J., Hieronymus,H. and Silver,P.A. (2004) Genome-wide localization of the nuclear transport machinery couples transcriptional status and nuclear organization. *Cell*, **117**, 427–439.
21. Chen,M. and Gartenberg,M.R. (2014) Coordination of tRNA transcription with export at nuclear pore complexes in budding yeast. *Genes Dev.*, **28**, 959–970.
22. Jacinto,F.V., Benner,C. and Hetzer,M.W. (2015) The nucleoporin Nup153 regulates embryonic stem cell pluripotency through gene silencing. *Genes Dev.*, **29**, 1224–1238.
23. Liang,Y. and Hetzer,M.W. (2011) Functional interactions between nucleoporins and chromatin. *Curr. Opin. Cell Biol.*, **23**, 65–70.
24. Ptak,C., Aitchison,J.D. and Wozniak,R.W. (2014) The multifunctional nuclear pore complex: a platform for controlling gene expression. *Curr. Opin. Cell Biol.*, **28**, 46–53.
25. Schmid,M., Arib,G., Laemmli,C., Nishikawa,J., Durussel,T. and Laemmli,U.K. (2006) Nup-PI: the nucleopore-promoter interaction of genes in yeast. *Mol. Cell*, **21**, 379–391.
26. Van de Vosse,D.W., Wan,Y., Lapetina,D.L., Chen,W.M., Chiang,J.H., Aitchison,J.D. and Wozniak,R.W. (2013) A role for the nucleoporin Nup170p in chromatin structure and gene silencing. *Cell*, **152**, 969–983.
27. Griffith,J.L., Coleman,L.E., Raymond,A.S., Goodson,S.G., Pittard,W.S., Tsui,C. and Devine,S.E. (2003) Functional genomics reveals relationships between the retrovirus-like Ty1 element and its host Saccharomyces cerevisiae. *Genetics*, **164**, 867–879.
28. Dakshinamurthy,A., Nyswaner,K.M., Farabaugh,P.J. and Garfinkel,D.J. (2010) BUD22 affects Ty1 retrotransposition and ribosome biogenesis in Saccharomyces cerevisiae. *Genetics*, **185**, 1193–1205.
29. Risler,J.K., Kenny,A.E., Palumbo,R.J., Gamache,E.R. and Curcio,M.J. (2012) Host co-factors of the retrovirus-like transposon Ty1. *Mob. DNA*, **3**, 12.
30. Chalker,D.L. and Sandmeyer,S.B. (1992) Ty3 integrates within the region of RNA polymerase III transcription initiation. *Genes Dev.*, **6**, 117–128.
31. Aye,M., Irwin,B., Beliakova-Bethell,N., Chen,E., Garrus,J. and Sandmeyer,S. (2004) Host factors that affect Ty3 retrotransposition in Saccharomyces cerevisiae. *Genetics*, **168**, 1159–1176.
32. Irwin,B., Aye,M., Baldi,P., Beliakova-Bethell,N., Cheng,H., Dou,Y., Liou,W. and Sandmeyer,S. (2005) Retroviruses and yeast

retrotransposons use overlapping sets of host genes. *Genome Res.*, **15**, 641–654.
33. Heath,C.V., Copeland,C.S., Amberg,D.C., Del Priore,V., Snyder,M. and Cole,C.N. (1995) Nuclear pore complex clustering and nuclear accumulation of poly(A)+ RNA associated with mutation of the Saccharomyces cerevisiae RAT2/NUP120 gene. *J. Cell Biol.*, **131**, 1677–1697.
34. Li,O., Heath,C.V., Amberg,D.C., Dockendorff,T.C., Copeland,C.S., Snyder,M. and Cole,C.N. (1995) Mutation or deletion of the Saccharomyces cerevisiae RAT3/NUP133 gene causes temperature-dependent nuclear accumulation of poly(A)+ RNA and constitutive clustering of nuclear pore complexes. *Mol. Biol. Cell*, **6**, 401–417.
35. Beliakova-Bethell,N., Terry,L.J., Bilanchone,V., DaSilva,R., Nagashima,K., Wente,S.R. and Sandmeyer,S. (2009) Ty3 nuclear entry is initiated by viruslike particle docking on GLFG nucleoporins. *J. Virol.*, **83**, 11914–11925.
36. Levin,H.L., Weaver,D.C. and Boeke,J.D. (1993) Novel gene expression mechanism in a fission yeast retroelement: Tf1 proteins are derived from a single primary translation product. *EMBO J.*, **12**, 4885–4895.
37. Teysset,L., Dang,V.D., Kim,M.K. and Levin,H.L. (2003) A long terminal repeat-containing retrotransposon of Schizosaccharomyces pombe expresses a Gag-like protein that assembles into virus-like particles which mediate reverse transcription. *J. Virol.*, **77**, 5451–5463.
38. Haag,A.L., Lin,J.H. and Levin,H.L. (2000) Evidence for the packaging of multiple copies of Tf1 mRNA into particles and the trans priming of reverse transcription. *J. Virol.*, **74**, 7164–7170.
39. Balasundaram,D., Benedik,M.J., Morphew,M., Dang,V.D. and Levin,H.L. (1999) Nup124p is a nuclear pore factor of Schizosaccharomyces pombe that is important for nuclear import and activity of retrotransposon Tf1. *Mol. Cell. Biol.*, **19**, 5768–5784.
40. Dang,V.D. and Levin,H.L. (2000) Nuclear import of the retrotransposon Tf1 is governed by a nuclear localization signal that possesses a unique requirement for the FXFG nuclear pore factor Nup124p. *Mol. Cell. Biol.*, **20**, 7798–7812.
41. Sistla,S., Pang,J.V., Wang,C.X. and Balasundaram,D. (2007) Multiple conserved domains of the nucleoporin Nup124p and its orthologs Nup1p and Nup153 are critical for nuclear import and activity of the fission yeast Tf1 retrotransposon. *Mol. Biol. Cell*, **18**, 3692–3708.
42. Varadarajan,P., Mahalingam,S., Liu,P., Ng,S.B., Gandotra,S., Dorairajoo,D.S. and Balasundaram,D. (2005) The functionally conserved nucleoporins Nup124p from fission yeast and the human Nup153 mediate nuclear import and activity of the Tf1 retrotransposon and HIV-1 Vpr. *Mol. Biol. Cell*, **16**, 1823–1838.
43. Brass,A.L., Dykxhoorn,D.M., Benita,Y., Yan,N., Engelman,A., Xavier,R.J., Lieberman,J. and Elledge,S.J. (2008) Identification of host proteins required for HIV infection through a functional genomic screen. *Science*, **319**, 921–926.
44. König,R., Zhou,Y., Elleder,D., Diamond,T.L., Bonamy,G.M., Irelan,J.T., Chiang,C.Y., Tu,B.P., De Jesus,P.D., Lilley,C.E. *et al.* (2008) Global analysis of host-pathogen interactions that regulate early-stage HIV-1 replication. *Cell*, **135**, 49–60.
45. Zhou,H., Xu,M., Huang,Q., Gates,A.T., Zhang,X.D., Castle,J.C., Stec,E., Ferrer,M., Strulovici,B., Hazuda,D.J. *et al.* (2008) Genome-scale RNAi screen for host factors required for HIV replication. *Cell Host Microbe*, **4**, 495–504.
46. Mészáros,N., Cibulka,J., Mendiburo,M.J., Romanauska,A., Schneider,M. and Köhler,A. (2015) Nuclear pore basket proteins are tethered to the nuclear envelope and can regulate membrane curvature. *Dev. Cell*, **33**, 285–298.
47. Dilworth,D.J., Suprapto,A., Padovan,J.C., Chait,B.T., Wozniak,R.W., Rout,M.P. and Aitchison,J.D. (2001) Nup2p dynamically associates with the distal regions of the yeast nuclear pore complex. *J. Cell Biol.*, **153**, 1465–1478.
48. Giaever,G., Chu,A.M., Ni,L., Connelly,C., Riles,L., Véronneau,S., Dow,S., Lucau-Danila,A., Anderson,K., André,B. *et al.* (2002) Functional profiling of the Saccharomyces cerevisiae genome. *Nature*, **418**, 387–391.
49. Li,Z., Vizeacoumar,F.J., Bahr,S., Li,J., Warringer,J., Vizeacoumar,F.S., Min,R., Vandersluis,B., Bellay,J., Devit,M. *et al.* (2011) Systematic exploration of essential yeast gene function with temperature-sensitive mutants. *Nat. Biotechnol.*, **29**, 361–367.
50. Curcio,M.J. and Garfinkel,D.J. (1991) Single-step selection for Ty1 element retrotransposition. *Proc. Natl. Acad. Sci. U.S.A.*, **88**, 936–940.
51. Nyswaner,K.M., Checkley,M.A., Yi,M., Stephens,R.M. and Garfinkel,D.J. (2008) Chromatin-associated genes protect the yeast genome from Ty1 insertional mutagenesis. *Genetics*, **178**, 197–214.
52. Walkey,C.J., Luo,Z., Madilao,L.L. and van Vuuren,H.J. (2012) The fermentation stress response protein Aaf1p/Yml081Wp regulates acetate production in Saccharomyces cerevisiae. *PLoS One*, **7**, e51551.
53. Fang,N.N., Ng,A.H., Measday,V. and Mayor,T. (2011) Hul5 HECT ubiquitin ligase plays a major role in the ubiquitylation and turnover of cytosolic misfolded proteins. *Nat. Cell Biol.*, **13**, 1344–1352.
54. Ho,K.L., Ma,L., Cheung,S., Manhas,S., Fang,N., Wang,K., Young,B., Loewen,C., Mayor,T. and Measday,V. (2015) A role for the budding yeast separase, Esp1, in Ty1 element retrotransposition. *PLos Genet.*, **11**, e1005109.
55. Sundararajan,A., Lee,B.S. and Garfinkel,D.J. (2003) The Rad27 (Fen-1) nuclease inhibits Ty1 mobility in Saccharomyces cerevisiae. *Genetics*, **163**, 55–67.
56. Lee,B.S., Lichtenstein,C.P., Faiola,B., Rinckel,L.A., Wysock,W., Curcio,M.J. and Garfinkel,D.J. (1998) Posttranslational inhibition of Ty1 retrotransposition by nucleotide excision repair/transcription factor TFIIH subunits Ssl2p and Rad3p. *Genetics*, **148**, 1743–1761.
57. Garfinkel,D.J., Nyswaner,K., Wang,J. and Cho,J.Y. (2003) Post-transcriptional cosuppression of Ty1 retrotransposition. *Genetics*, **165**, 83–99.
58. Dilworth,D.J., Tackett,A.J., Rogers,R.S., Yi,E.C., Christmas,R.H., Smith,J.J., Siegel,A.F., Chait,B.T., Wozniak,R.W. and Aitchison,J.D. (2005) The mobile nucleoporin Nup2p and chromatin-bound Prp20p function in endogenous NPC-mediated transcriptional control. *J. Cell Biol.*, **171**, 955–965.
59. Ishii,K., Arib,G., Lin,C., Van Houwe,G. and Laemmli,U.K. (2002) Chromatin boundaries in budding yeast: the nuclear pore connection. *Cell*, **109**, 551–562.
60. Melamed,C., Nevo,Y. and Kupiec,M. (1992) Involvement of cDNA in homologous recombination between Ty elements in Saccharomyces cerevisiae. *Mol. Cell. Biol.*, **12**, 1613–1620.
61. Winston,F., Durbin,K.J. and Fink,G.R. (1984) The SPT3 gene is required for normal transcription of Ty elements in S. cerevisiae. *Cell*, **39**, 675–682.
62. Mularoni,L., Zhou,Y., Bowen,T., Gangadharan,S., Wheelan,S.J. and Boeke,J.D. (2012) Retrotransposon Ty1 integration targets specifically positioned asymmetric nucleosomal DNA segments in tRNA hotspots. *Genome Res.*, **22**, 693–703.
63. Baller,JA, Gao,J, Stamenova,R, Curcio,MJ and Voytas,DF (2012) A nucleosomal surface defines an integration hotspot for the Saccharomyces cerevisiae Ty1 retrotransposon. *Genome Res.*, **22** 704–13
64. Ji,H., Moore,D.P., Blomberg,M.A., Braiterman,L.T., Voytas,D.F., Natsoulis,G. and Boeke,J.D. (1993) Hotspots for unselected Ty1 transposition events on yeast chromosome III are near tRNA genes and LTR sequences. *Cell*, **73**, 1007–1018.
65. Bloom,K.S. (2014) Centromeric heterochromatin: the primordial segregation machine. *Annu. Rev. Genet.*, **48**, 457–484.
66. Snider,C.E., Stephens,A.D., Kirkland,J.G., Hamdani,O., Kamakaka,R.T. and Bloom,K. (2014) Dyskerin, tRNA genes, and condensin tether pericentric chromatin to the spindle axis in mitosis. *J. Cell Biol.*, **207**, 189–199.
67. Anderson,J.T., Wilson,S.M., Datar,K.V. and Swanson,M.S. (1993) NAB2: a yeast nuclear polyadenylated RNA-binding protein essential for cell viability. *Mol. Cell. Biol.*, **13**, 2730–2741.
68. Soucek,S., Corbett,A.H. and Fasken,M.B. (2012) The long and the short of it: the role of the zinc finger polyadenosine RNA binding protein, Nab2, in control of poly(A) tail length. *Biochim. Biophys. Acta*, **1819**, 546–554.
69. Green,D.M., Johnson,C.P., Hagan,H. and Corbett,A.H. (2003) The C-terminal domain of myosin-like protein 1 (Mlp1p) is a docking site for heterogeneous nuclear ribonucleoproteins that are required for mRNA export. *Proc. Natl. Acad. Sci. U.S.A.*, **100**, 1010–1015.
70. Grant,R.P., Marshall,N.J., Yang,J.C., Fasken,M.B., Kelly,S.M., Harreman,M.T., Neuhaus,D., Corbett,A.H. and Stewart,M. (2008)

Structure of the N-terminal Mlp1-binding domain of the Saccharomyces cerevisiae mRNA-binding protein, Nab2. *J. Mol. Biol.*, **376**, 1048–1059.
71. Fasken,M.B., Stewart,M. and Corbett,A.H. (2008) Functional significance of the interaction between the mRNA-binding protein, Nab2, and the nuclear pore-associated protein, Mlp1, in mRNA export. *J. Biol. Chem.*, **283**, 27130–27143.
72. Reuter,L.M., Meinel,D.M. and Sträßer,K. (2015) The poly(A)-binding protein Nab2 functions in RNA polymerase III transcription. *Genes Dev.*, **29**, 1565–1575.
73. Rout,M.P., Aitchison,J.D., Suprapto,A., Hjertaas,K., Zhao,Y. and Chait,B.T. (2000) The yeast nuclear pore complex: composition, architecture, and transport mechanism. *J. Cell Biol.*, **148**, 635–651.
74. Fischer,T., Strässer,K., Rácz,A., Rodriguez-Navarro,S., Oppizzi,M., Ihrig,P., Lechner,J. and Hurt,E. (2002) The mRNA export machinery requires the novel Sac3p-Thp1p complex to dock at the nucleoplasmic entrance of the nuclear pores. *EMBO J.*, **21**, 5843–5852.
75. Sharma,K., Fabre,E., Tekotte,H., Hurt,E.C. and Tollervey,D. (1996) Yeast nucleoporin mutants are defective in pre-tRNA splicing. *Mol. Cell. Biol.*, **16**, 294–301.
76. Yoshihisa,T., Yunoki-Esaki,K., Ohshima,C., Tanaka,N. and Endo,T. (2003) Possibility of cytoplasmic pre-tRNA splicing: the yeast tRNA splicing endonuclease mainly localizes on the mitochondria. *Mol. Biol. Cell*, **14**, 3266–3279.
77. Burns,L.T. and Wente,S.R. (2014) From hypothesis to mechanism: uncovering nuclear pore complex links to gene expression. *Mol. Cell. Biol.*, **34**, 2114–2120.
78. Raices,M. and D'Angelo,M.A. (2017) Nuclear pore complexes and regulation of gene expression. *Curr. Opin. Cell Biol.*, **46**, 26–32.
79. Hayakawa,A., Babour,A., Sengmanivong,L. and Dargemont,C. (2012) Ubiquitylation of the nuclear pore complex controls nuclear migration during mitosis in S. cerevisiae. *J. Cell Biol.*, **196**, 19–27.
80. Niño,C.A., Guet,D., Gay,A., Brutus,S., Jourquin,F., Mendiratta,S., Salamero,J., Géli,V. and Dargemont,C. (2016) Posttranslational marks control architectural and functional plasticity of the nuclear pore complex basket. *J. Cell Biol.*, **212**, 167–180.
81. Horigome,C., Bustard,D.E., Marcomini,I., Delgoshaie,N., Tsai-Pflugfelder,M., Cobb,J.A. and Gasser,S.M. (2016) PolySUMOylation by Siz2 and Mms21 triggers relocation of DNA breaks to nuclear pores through the Slx5/Slx8 STUbL. *Genes Dev.*, **30**, 931–945.
82. Terry,L.J. and Wente,S.R. (2009) Flexible gates: dynamic topologies and functions for FG nucleoporins in nucleocytoplasmic transport. *Eukaryot Cell*, **8**, 1814–1827.
83. Hülsmann,B.B., Labokha,A.A. and Görlich,D. (2012) The permeability of reconstituted nuclear pores provides direct evidence for the selective phase model. *Cell*, **150**, 738–751.
84. Finn,E.M., DeRoo,E.P., Clement,G.W., Rao,S., Kruse,S.E., Kokanovich,K.M. and Belanger,K.D. (2013) A subset of FG-nucleoporins is necessary for efficient Msn5-mediated nuclear protein export. *Biochim. Biophys. Acta*, **1833**, 1096–1103.
85. Strawn,L.A., Shen,T., Shulga,N., Goldfarb,D.S. and Wente,S.R. (2004) Minimal nuclear pore complexes define FG repeat domains essential for transport. *Nat. Cell Biol.*, **6**, 197–206.
86. Li,C., Goryaynov,A. and Yang,W. (2016) The selective permeability barrier in the nuclear pore complex. *Nucleus*, **7**, 430–446.
87. Rout,M.P. and Wente,S.R. (1994) Pores for thought: nuclear pore complex proteins. *Trends Cell Biol.*, **4**, 357–365.
88. Adams,R.L., Terry,L.J. and Wente,S.R. (2015) A Novel Saccharomyces cerevisiae FG Nucleoporin Mutant Collection for Use in Nuclear Pore Complex Functional Experiments. *G3 (Bethesda)*, **6**, 51–58.
89. Solsbacher,J., Maurer,P., Vogel,F. and Schlenstedt,G. (2000) Nup2p, a yeast nucleoporin, functions in bidirectional transport of importin alpha. *Mol. Cell. Biol.*, **20**, 8468–8479.
90. Allen,N.P., Huang,L., Burlingame,A. and Rexach,M. (2001) Proteomic analysis of nucleoporin interacting proteins. *J. Biol. Chem.*, **276**, 29268–29274.
91. Hood,J.K., Casolari,J.M. and Silver,P.A. (2000) Nup2p is located on the nuclear side of the nuclear pore complex and coordinates Srp1p/importin-alpha export. *J. Cell Sci.*, **113**(Pt 8), 1471–1480.
92. Booth,J.W., Belanger,K.D., Sannella,M.I. and Davis,L.I. (1999) The yeast nucleoporin Nup2p is involved in nuclear export of importin alpha/Srp1p. *J. Biol. Chem.*, **274**, 32360–32367.
93. Belanger,K.D., Kenna,M.A., Wei,S. and Davis,L.I. (1994) Genetic and physical interactions between Srp1p and nuclear pore complex proteins Nup1p and Nup2p. *J. Cell Biol.*, **126**, 619–630.
94. Rexach,M. and Blobel,G. (1995) Protein import into nuclei: association and dissociation reactions involving transport substrate, transport factors, and nucleoporins. *Cell*, **83**, 683–692.
95. Loeb,J.D., Davis,L.I. and Fink,G.R. (1993) NUP2, a novel yeast nucleoporin, has functional overlap with other proteins of the nuclear pore complex. *Mol. Biol. Cell*, **4**, 209–222.
96. Denning,D., Mykytka,B., Allen,N.P., Huang,L., Burlingame,Al and Rexach,M. (2001) The nucleoporin Nup60p functions as a Gsp1p-GTP-sensitive tether for Nup2p at the nuclear pore complex. *J. Cell Biol.*, **154**, 937–950.
97. Dingwall,C., Kandels-Lewis,S. and Séraphin,B. (1995) A family of Ran binding proteins that includes nucleoporins. *Proc. Natl. Acad. Sci. U.S.A.*, **92**, 7525–7529.
98. Köhler,A. and Hurt,E. (2007) Exporting RNA from the nucleus to the cytoplasm. *Nat. Rev. Mol. Cell Biol.*, **8**, 761–773.
99. Chávez,S., Beilharz,T., Rondón,A.G., Erdjument-Bromage,H., Tempst,P., Svejstrup,J.Q., Lithgow,T. and Aguilera,A. (2000) A protein complex containing Tho2, Hpr1, Mft1 and a novel protein, Thp2, connects transcription elongation with mitotic recombination in Saccharomyces cerevisiae. *EMBO J.*, **19**, 5824–5834.
100. Strässer,K., Masuda,S., Mason,P., Pfannstiel,J., Oppizzi,M., Rodriguez-Navarro,S., Rondón,A.G., Aguilera,A., Struhl,K., Reed,R. *et al.* (2002) TREX is a conserved complex coupling transcription with messenger RNA export. *Nature*, **417**, 304–308.
101. Peña,A., Gewartowski,K., Mroczek,S., Cuéllar,J., Szykowska,A., Prokop,A., Czarnocki-Cieciura,M., Piwowarski,J., Tous,C., Aguilera,A. *et al.* (2012) Architecture and nucleic acids recognition mechanism of the THO complex, an mRNP assembly factor. *EMBO J.*, **31**, 1605–1616.
102. Rondón,A.G., Jimeno,S., García-Rubio,M. and Aguilera,A. (2003) Molecular evidence that the eukaryotic THO/TREX complex is required for efficient transcription elongation. *J. Biol. Chem.*, **278**, 39037–39043.
103. Meinel,D.M. and Sträßer,K. (2015) Co-transcriptional mRNP formation is coordinated within a molecular mRNP packaging station in S. cerevisiae. *Bioessays*, **37**, 666–677.
104. Gwizdek,C., Hobeika,M., Kus,B., Ossareh-Nazari,B., Dargemont,C. and Rodriguez,M.S. (2005) The mRNA nuclear export factor Hpr1 is regulated by Rsp5-mediated ubiquitylation. *J. Biol. Chem.*, **280**, 13401–13405.
105. Aguilera,A. and Klein,H.L. (1990) HPR1, a novel yeast gene that prevents intrachromosomal excision recombination, shows carboxy-terminal homology to the Saccharomyces cerevisiae TOP1 gene. *Mol. Cell. Biol.*, **10**, 1439–1451.
106. Santos-Rosa,H. and Aguilera,A. (1994) Increase in incidence of chromosome instability and non-conservative recombination between repeats in Saccharomyces cerevisiae hpr1 delta strains. *Mol. Gen. Genet.*, **245**, 224–236.
107. García-Oliver,E., García-Molinero,V. and Rodríguez-Navarro,S. (2012) mRNA export and gene expression: the SAGA-TREX-2 connection. *Biochim. Biophys. Acta*, **1819**, 555–565.
108. Rondón,A.G., Jimeno,S. and Aguilera,A. (2010) The interface between transcription and mRNP export: from THO to THSC/TREX-2. *Biochim. Biophys. Acta*, **1799**, 533–538.
109. Fischer,T., Rodríguez-Navarro,S., Pereira,G., Rácz,A., Schiebel,E. and Hurt,E. (2004) Yeast centrin Cdc31 is linked to the nuclear mRNA export machinery. *Nat. Cell Biol.*, **6**, 840–848.
110. Rodríguez-Navarro,S., Fischer,T., Luo,M.J., Antúnez,O., Brettschneider,S., Lechner,J., Pérez-Ortín,J.E., Reed,R. and Hurt,E. (2004) Sus1, a functional component of the SAGA histone acetylase complex and the nuclear pore-associated mRNA export machinery. *Cell*, **116**, 75–86.
111. Cabal,G.G., Genovesio,A., Rodriguez-Navarro,S., Zimmer,C., Gadal,O., Lesne,A., Buc,H., Feuerbach-Fournier,F., Olivo-Marin,J.C., Hurt,E.C. *et al.* (2006) SAGA interacting factors confine sub-diffusion of transcribed genes to the nuclear envelope. *Nature*, **441**, 770–773.

112. Bermejo,R., Capra,T., Jossen,R., Colosio,A., Frattini,C., Carotenuto,W., Cocito,A., Doksani,Y., Klein,H., Gómez-González,B. *et al.* (2011) The replication checkpoint protects fork stability by releasing transcribed genes from nuclear pores. *Cell*, **146**, 233–246.
113. González-Aguilera,C., Tous,C., Gómez-González,B., Huertas,P., Luna,R. and Aguilera,A. (2008) The THP1-SAC3-SUS1-CDC31 complex works in transcription elongation-mRNA export preventing RNA-mediated genome instability. *Mol. Biol. Cell*, **19**, 4310–4318.
114. Jani,D., Lutz,S., Marshall,N.J., Fischer,T., Köhler,A., Ellisdon,A.M., Hurt,E. and Stewart,M. (2009) Sus1, Cdc31, and the Sac3 CID region form a conserved interaction platform that promotes nuclear pore association and mRNA export. *Mol. Cell*, **33**, 727–737.
115. Blobel,G. (1985) Gene gating: a hypothesis. *Proc. Natl. Acad. Sci. U.S.A.*, **82**, 8527–8529.
116. Dieppois,G., Iglesias,N. and Stutz,F. (2006) Cotranscriptional recruitment to the mRNA export receptor Mex67p contributes to nuclear pore anchoring of activated genes. *Mol. Cell. Biol.*, **26**, 7858–7870.
117. Brickner,J.H. and Walter,P. (2004) Gene recruitment of the activated INO1 locus to the nuclear membrane. *PLoS Biol.*, **2**, e342.
118. Taddei,A., Van Houwe,G., Hediger,F., Kalck,V., Cubizolles,F., Schober,H. and Gasser,S.M. (2006) Nuclear pore association confers optimal expression levels for an inducible yeast gene. *Nature*, **441**, 774–778.
119. Kalverda,B. and Fornerod,M. (2010) Characterization of genome-nucleoporin interactions in Drosophila links chromatin insulators to the nuclear pore complex. *Cell Cycle*, **9**, 4812–4817.
120. Vaquerizas,J.M., Suyama,R., Kind,J., Miura,K., Luscombe,N.M. and Akhtar,A. (2010) Nuclear pore proteins nup153 and megator define transcriptionally active regions in the Drosophila genome. *PLos Genet.*, **6**, e1000846.
121. Liang,Y., Franks,T.M., Marchetto,M.C., Gage,F.H. and Hetzer,M.W. (2013) Dynamic association of NUP98 with the human genome. *PLos Genet.*, **9**, e1003308.
122. Light,W.H., Brickner,D.G., Brand,V.R. and Brickner,J.H. (2010) Interaction of a DNA zip code with the nuclear pore complex promotes H2A.Z incorporation and INO1 transcriptional memory. *Mol. Cell*, **40**, 112–125.
123. Menon,B.B., Sarma,N.J., Pasula,S., Deminoff,S.J., Willis,K.A., Barbara,K.E., Andrews,B. and Santangelo,G.M. (2005) Reverse recruitment: the Nup84 nuclear pore subcomplex mediates Rap1/Gcr1/Gcr2 transcriptional activation. *Proc. Natl. Acad. Sci. U.S.A.*, **102**, 5749–5754.
124. Simos,G., Tekotte,H., Grosjean,H., Segref,A., Sharma,K., Tollervey,D. and Hurt,E.C. (1996) Nuclear pore proteins are involved in the biogenesis of functional tRNA. *EMBO J.*, **15**, 2270–2284.
125. Wu,J., Bao,A., Chatterjee,K., Wan,Y. and Hopper,A.K. (2015) Genome-wide screen uncovers novel pathways for tRNA processing and nuclear-cytoplasmic dynamics. *Genes Dev.*, **29**, 2633–2644.
126. Pamblanco,M., Oliete-Calvo,P., García-Oliver,E., Luz Valero,M., Sanchez del Pino,M.M. and Rodríguez-Navarro,S. (2014) Unveiling novel interactions of histone chaperone Asf1 linked to TREX-2 factors Sus1 and Thp1. *Nucleus*, **5**, 247–259.
127. Aitchison,J.D., Blobel,G. and Rout,M.P. (1995) Nup120p: a yeast nucleoporin required for NPC distribution and mRNA transport. *J. Cell Biol.*, **131**, 1659–1675.
128. Doye,V., Wepf,R. and Hurt,E.C. (1994) A novel nuclear pore protein Nup133p with distinct roles in poly(A)+ RNA transport and nuclear pore distribution. *EMBO J.*, **13**, 6062–6075.
129. Pemberton,L.F., Rout,M.P. and Blobel,G. (1995) Disruption of the nucleoporin gene NUP133 results in clustering of nuclear pore complexes. *Proc. Natl. Acad. Sci. U.S.A.*, **92**, 1187–1191.
130. Zabel,U., Doye,V., Tekotte,H., Wepf,R., Grandi,P. and Hurt,E.C. (1996) Nic96p is required for nuclear pore formation and functionally interacts with a novel nucleoporin, Nup188p. *J. Cell Biol.*, **133**, 1141–1152.
131. Stephan,A.K., Kliszczak,M. and Morrison,C.G. (2011) The Nse2/Mms21 SUMO ligase of the Smc5/6 complex in the maintenance of genome stability. *FEBS Lett.*, **585**, 2907–2913.
132. Jalal,D., Chalissery,J. and Hassan,A.H. (2017) Genome maintenance in Saccharomyces cerevisiae: the role of SUMO and SUMO-targeted ubiquitin ligases. *Nucleic. Acids. Res.*, **45**, 2242–2261.
133. Chymkowitch,P., Nguéa,P.A., Aanes,H., Robertson,J., Klungland,A. and Enserink,J.M. (2017) TORC1-dependent sumoylation of Rpc82 promotes RNA polymerase III assembly and activity. *Proc. Natl. Acad. Sci. U.S.A.*, **114**, 1039–1044.
134. Chymkowitch,P. and Enserink,J.M. (2017) Regulation of tRNA synthesis by posttranslational modifications of RNA polymerase III subunits. *Biochim. Biophys. Acta*, doi:10.1016/j.bbagrm.2017.11.001.
135. Brickner,D.G., Ahmed,S., Meldi,L., Thompson,A., Light,W., Young,M., Hickman,T.L., Chu,F., Fabre,E. and Brickner,J.H. (2012) Transcription factor binding to a DNA zip code controls interchromosomal clustering at the nuclear periphery. *Dev. Cell*, **22**, 1234–1246.
136. Hellmuth,K., Lau,D.M., Bischoff,F.R., Künzler,M., Hurt,E. and Simos,G. (1998) Yeast Los1p has properties of an exportin-like nucleocytoplasmic transport factor for tRNA. *Mol. Cell. Biol.*, **18**, 6374–6386.
137. Matreyek,K.A. and Engelman,A. (2013) Viral and cellular requirements for the nuclear entry of retroviral preintegration nucleoprotein complexes. *Viruses*, **5**, 2483–2511.
138. Matreyek,K.A., Yücel,S.S., Li,X. and Engelman,A. (2013) Nucleoporin NUP153 phenylalanine-glycine motifs engage a common binding pocket within the HIV-1 capsid protein to mediate lentiviral infectivity. *PLoS Pathog.*, **9**, e1003693.
139. Matreyek,K.A. and Engelman,A. (2011) The requirement for nucleoporin NUP153 during human immunodeficiency virus type 1 infection is determined by the viral capsid. *J. Virol.*, **85**, 7818–7827.
140. Marini,B., Kertesz-Farkas,A., Ali,H., Lucic,B., Lisek,K., Manganaro,L., Pongor,S., Luzzati,R., Recchia,A., Mavilio,F. *et al.* (2015) Nuclear architecture dictates HIV-1 integration site selection. *Nature*, **521**, 227–231.
141. Lelek,M., Casartelli,N., Pellin,D., Rizzi,E., Souque,P., Severgnini,M., Di Serio,C., Fricke,T., Diaz-Griffero,F., Zimmer,C. *et al.* (2015) Chromatin organization at the nuclear pore favours HIV replication. *Nat. Commun.*, **6**, 6483.
142. Burdick,R.C., Hu,W.S. and Pathak,V.K. (2013) Nuclear import of APOBEC3F-labeled HIV-1 preintegration complexes. *Proc. Natl. Acad. Sci. U.S.A.*, **110**, E4780–E4789.
143. Di Primio,C., Quercioli,V., Allouch,A., Gijsbers,R., Christ,F., Debyser,Z., Arosio,D. and Cereseto,A. (2013) Single-cell imaging of HIV-1 provirus (SCIP). *Proc. Natl. Acad. Sci. U.S.A.*, **110**, 5636–5641.